

# Climate adaptation Colombia

## Climate data scaling and analysis for the Magdalena basin

July 2014

### Authors

Philip Kraaijenbrink  
Arthur Lutz  
Peter Droogers

### Client

Partners voor Water

### Report FutureWater

128



### FutureWater

Costerweg 1V  
6702 AA Wageningen  
The Netherlands

+31 (0)317 460050

[info@futurewater.nl](mailto:info@futurewater.nl)

[www.futurewater.nl](http://www.futurewater.nl)

# Preface

The Netherlands' "Partners for Water" initiative has the objective to support the Dutch water sector to capitalize on its technologies and expertise internationally, while simultaneously ensure that Dutch technologies and knowledge contribute to solving world water challenges.

A call for a proposal was announced by "Partners for Water" 2013. A consortium of four Dutch partners developed a proposal on request of IDEAM (Instituto de Hidrología, Meteorología y Estudios Ambientales de Colombia), Bogotá, Colombia, under the name "Climate adaptation Colombia: a tipping point analysis".

The contract number is *PVWS13023*.

The project partners are:

- Deltares, Utrecht, Netherlands (lead)
- UNESCO-IHE, Delft, Netherlands
- SarVision, Wageningen, Netherlands
- FutureWater, Wageningen, Netherlands
- Waterschap Hunze en Aa's, Veendam, Netherlands
- IDEAM, Bogotá, Colombia
- DNP, Bogota, Colombia
- CorMagdalena, Bogotá, Colombia



# Table of contents

<b>1</b>	<b>Introduction</b>	<b>1</b>
1.1	Project background	1
1.2	Objectives	1
1.3	The Magdalena River basin	2
<b>2</b>	<b>Baseline climate data</b>	<b>3</b>
2.1	Introduction	3
2.2	Records of in situ ground observations	3
2.2.1	Global Summary of the Day	3
2.2.2	IDEAM meteorological stations	3
2.3	Gridded meteorological datasets	4
2.3.1	Gridded datasets based solely on observations	6
2.3.2	Gridded reanalysis datasets	7
2.3.3	Other products	11
2.4	Selection of a dataset	12
2.5	Downscaling of gridded data to modelling scale	15
<b>3</b>	<b>Future climate data</b>	<b>17</b>
3.1	Introduction	17
3.1.1	Interpolation of global climate model data	17
3.1.2	Transformation of historical series	17
3.2	Global climate models	18
3.2.1	GCMs, CMIP5 and RCPs background	18
3.2.2	Climate periods of interest	19
3.2.3	Selection of GCMs and model realizations	19
3.3	Advanced delta change method	20
3.4	Temperature transformation	23
<b>4</b>	<b>Climate trends</b>	<b>24</b>
4.1	Baseline climate 1979-2008	24
4.1.1	Inter-annual trends	24
4.1.2	Intra-annual trends	26
4.1.3	Precipitation return periods	27
4.1.4	Spatial distribution of precipitation	28
4.1.5	Spatial distribution of temperature and evapotranspiration	28
4.2	Future changes in climate	30
4.2.1	Changes in precipitation distribution	30
4.2.2	Changes in temperature	34
4.2.3	Changes in reference evapotranspiration	34
4.2.4	Return period changes	36
4.2.5	Spatial changes	36
<b>5</b>	<b>References</b>	<b>39</b>



# Tables

Table 1. Gridded meteorological data products available for the Magdalena basin.....	5
Table 2. Scores for selection criteria for observation-based products.....	14
Table 3. Scores for selection criteria for reanalysis products.....	14
Table 4. Examined GCM realizations.....	19

# Figures

Figure 1. Location of the Magdalena river basin in North-West Colombia.....	2
Figure 2. GSOD stations and IDEAM stations in the Magdalena basin area.....	4
Figure 3. The three different grid scales used in this project.....	15
Figure 4. Example of a time step of the original and downscaled PRINCETON data.....	16
Figure 5. The RCPs and the four 30-year climate periods used in this project.....	18
Figure 6. Schematic examples of precipitation distributions used for the advanced delta change method.....	21
Figure 7. Flowchart overview of the steps performed to apply the advanced delta change method.....	22
Figure 8. Annual precipitation and mean temperature for the PRINCETON 1979-2008 data series.....	24
Figure 9. Indicator of the strength of the El Niño Southern Oscillation; the monthly oceanic niño index.....	25
Figure 10. Boxplots of daily precipitation.....	26
Figure 11. Boxplots of daily mean temperature.....	27
Figure 12. Boxplots of daily reference evapotranspiration.....	27
Figure 13. Return levels and periods of basin average daily precipitation.....	28
Figure 14. Seasonal maps for precipitation, temperature and estimated reference evapotranspiration.....	29
Figure 15. Basin average changes in $P_{30}$ , $P_{60}$ and $P_{90}$ for the transformed PRINCETON series.....	31
Figure 16. Basin average changes for the PRINCETON series transformed with HadGEM2-ES r1i1p1.....	32
Figure 17. Basin average changes for the PRINCETON series transformed with MPI-ESM-LR r2i1p1.....	33
Figure 18. Basin average changes in minimum, average and maximum temperature for the transformed data..	35
Figure 19. Return periods and return levels for basin average precipitation of the future scenarios.....	36
Figure 20. Spatial variability of the differences for MPI-ESM-LR RCP 4.5 2071-2100.....	37
Figure 21. Spatial variability of the differences for HadGEM2-ES RCP 8.5 2071-2100.....	38



# 1 Introduction

## 1.1 Project background<sup>1</sup>

In the nineties of the last century Colombian governmental and research institutes have been working on many environmental policies and conservation initiatives. To study topics such as Greenhouse Gas emissions, glacier melt, coastal safety and water resource management, these initiatives required the prediction and mitigation of potential future changes in climate and its implications on ecosystems, agriculture, human and animal health, industry and infrastructure (IDEAM, 2001, 2010). There was a continuation of this line of research, which was largely executed under the United Nations Framework Convention on Climate Change (UNFCCC), in the first decade of this century. As was the case with general climate change research, the continued research line experienced a slight shift in focus towards more quantitative analyses as climate models gradually improved (IDEAM, 2010).

In 2011 Colombia was severely hit by large inundations, primarily due to flooding of the Magdalena River. This triggered the Colombian government and water institutions to enforce the attention given to water security and dike safety. This opened opportunities for the Netherlands with its knowledge developed during its long history in water management in the form of the research project "*Climate adaptation Colombia: A Tipping Point Analysis*", which is part of the Dutch *Partners voor Water* framework:

Recently project partner Deltares developed an approach for the analysis of climate adaptation options, the so called Adaptation Tipping Points. These tipping points in combination with Adaptation Pathways are major elements of the climate adaptation approach. The use of this adaptation tipping point approach will aid in identification of policy implications and it can be the foundation for actionable recommendations. These will comprise recommended adaptation actions in terms of flood risks and water availability that will ideally be input for Colombian policy plans and agendas.

An important part of the tipping point analysis is the development of a hydrological model of the Magdalena River system by Deltares that has a 0.02° resolution and is built within the open source PCRaster software (Utrecht University, 2013). The model is optimized by using historical discharge measurements as well as flood extent maps and land use information delivered by project partner SarVision. The calibration of the model will be performed using historical daily datasets of precipitation and reference evapotranspiration. To assess future changes in discharge extremes the downscaled climate data sets of the Coupled Model Intercomparison Project Phase 5 (CMIP5) will be used to force the hydrological model.

## 1.2 Objectives<sup>1</sup>

One of FutureWater's strengths lies in performing past and future climate data analyses, climate model interpretations and climate data downscaling for practical and applied purposes. Hence, in the framework of the *Partners voor Water* project FutureWater was assigned to do deliver the required historical climate data as well as to determine the future climate projections for the Magdalena river basin. This report describes the methods and findings of this assignment.

---

<sup>1</sup> Partly obtained from the Partners voor Water proposal "*Climate Adaptation Colombia: A Tipping Points Analysis*".



The objectives of FutureWater in this project are to:

- Evaluate the availability and quality of various historical data sources
- Downscale and convert historical data to the modelling scale and data format
- Perform downscaling of selected CMIP5 climate model data ziekteverspreiding
- Analyze historical climate trends and the future changes in climate provided by the scenarios

### 1.3 The Magdalena River basin

The study area for this project is the Magdalena River basin located in Colombia, which is South America's fifth largest basin. The Magdalena River originates in the Northern Andes Mountains and flows through almost every Andean ecosystem, from cloud forests to coastal lagoons. Once it leaves the Andes chains, the Magdalena River suffers a sudden change of slope in a vast region known as the Momposina Depression, which forms one of the biggest internal deltas of the world. It is localized in the zone where large part of agriculture and cattle farming takes place. Its basin covers 24% of Colombia's national territory, generating life and acting as an economic life force for more than 30 million Colombians living throughout the basin. The Magdalena flows for roughly 1500 kilometres, making it the principal artery of the country and a connection to the Caribbean (Great Rivers Partnership, 2014).

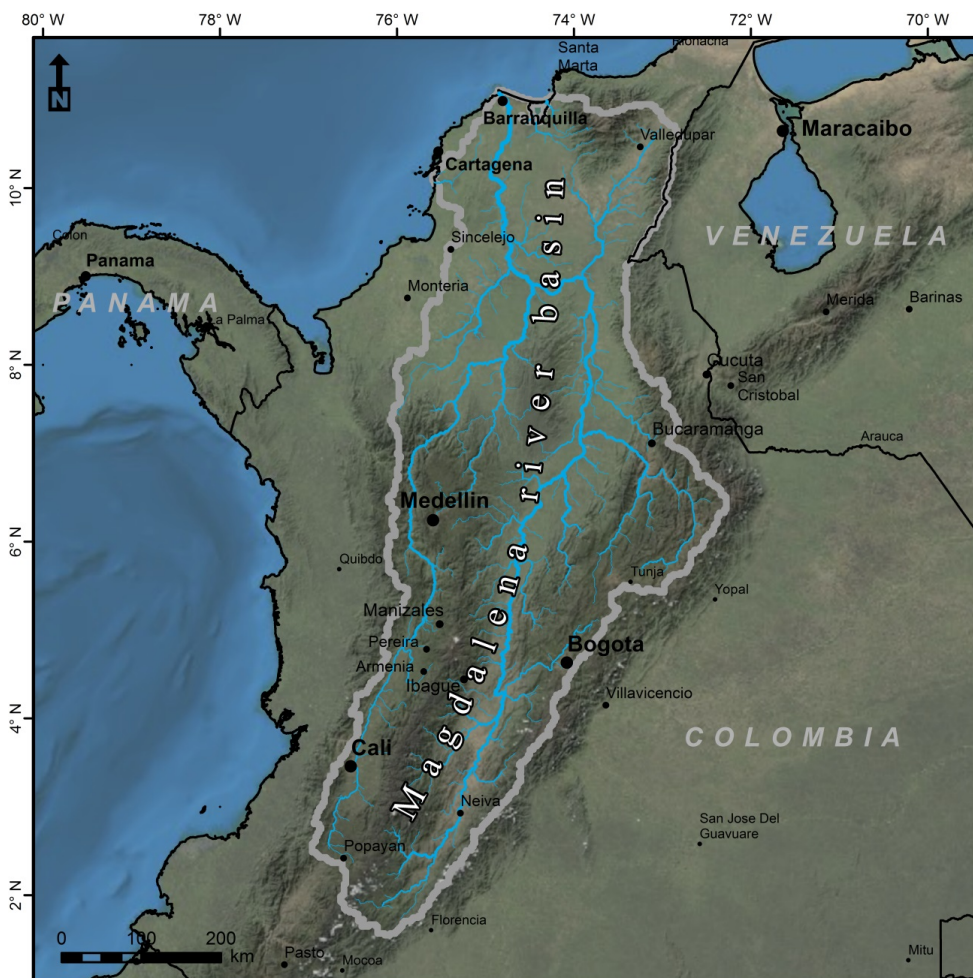


Figure 1. Location of the Magdalena river basin in North-West Colombia, enclosed by the Northern Andes mountain ranges and foothills and flowing into the Caribbean Sea.



## 2 Baseline climate data

### 2.1 Introduction

Different sources of meteorological data for the two main climatic parameters, i.e. precipitation and air temperature, can be found that could be used as baseline climate for further analysis (Lutz et al., 2014). Air temperature products are based on in situ measured observations and/or climatic models. Currently no reliable remote sensing products are available to estimate near surface air temperature. In general three groups of products can be distinguished to obtain air temperature data:

- Records of in situ observations
- Gridded products based on interpolation of in situ observed data
- Gridded reanalysis datasets

Understanding the spatial and temporal variability of precipitation in tropical areas remains a key challenge. Point measurements are often not sufficient to capture the strong gradients in the multiple local factors that determine the distribution of precipitation. Remote sensing data is currently providing a new venue for a better quantification of rainfall patterns. Rainfall satellite products are being continuously improved and increasing amounts of remote sensing data are becoming available for indirect indicators for the spatial distribution of precipitation. Four groups of precipitation products can be distinguished:

- Records of in situ observations
- Gridded products based on interpolation of in situ rain gauge data (e.g. APHRODITE, GPCC, CRU)
- Gridded satellite products based on the merging of different remote-sensing and ground-control data (e.g. TRMM, GPCP)
- Gridded reanalysis products (e.g. ERA (Interim/40/15/20CM))

### 2.2 Records of in situ ground observations

#### 2.2.1 Global Summary of the Day

Within the Magdalena basin daily meteorological ground observations of precipitation and temperature (daily mean, maximum and minimum) are available from the World Meteorological Organization's Global Summary of the Day (GSOD) database. The accuracy of these measured data is assumed to be high and could in theory be used for interpolation to the modelling grid or to perform bias-corrections of gridded datasets after interpolation. However, the abundance of meteorological stations in and near the Magdalena basin is low; there are a total of 35 stations found that have data available within the 1981-2010 period (Figure 2, left panel). Many of the stations in the area also have records that are far from complete, which renders the dataset unusable for the objectives of this project.

#### 2.2.2 IDEAM meteorological stations

The Institute of Hydrology, Meteorology and Environmental Studies (IDEAM) in Colombia maintains (a dataset of) over 8000 meteorological stations in Colombia (pers. comm.). The



stations are well distributed over the Magdalena basin area (Figure 2, right panel) and they would be very useful as climate input for hydrological modelling. It is unknown what the data time spans of specific stations are but there is confidence that enough stations are available for the entire chosen reference period in order to perform an interpolation procedure with accurate results. Unfortunately, the data acquisition was not successful within the project timeframe, which resulted in a forced utilization of other, likely less accurate, data sources.<sup>1</sup>

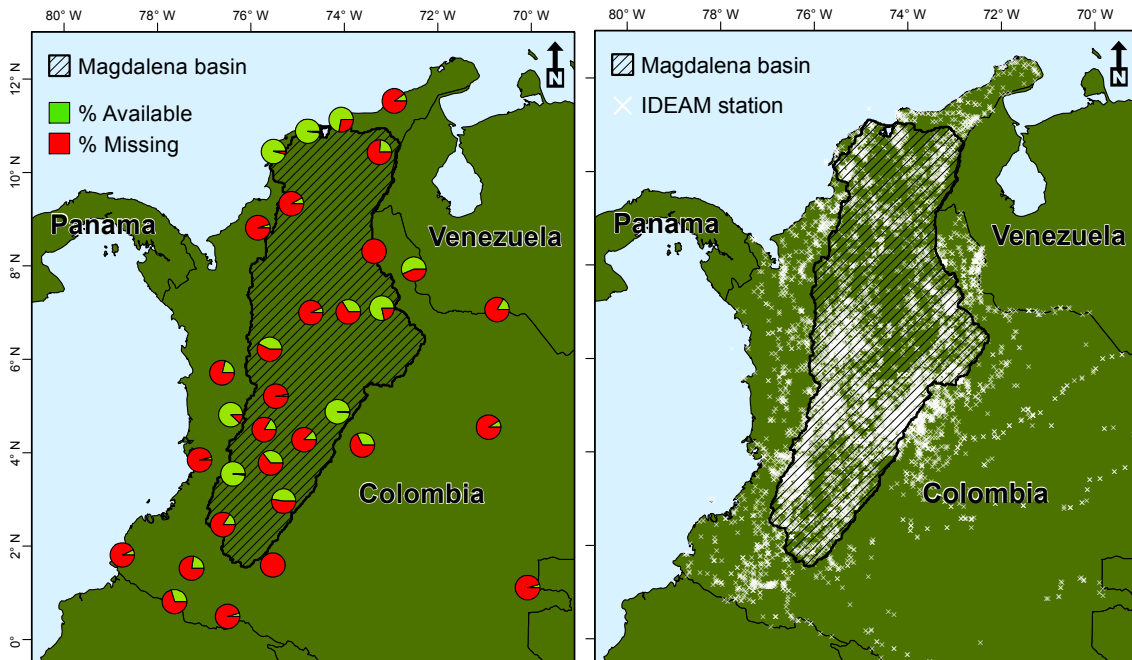


Figure 2. GSOD stations available for the Magdalena basin area and the completeness of their 1981-2010 data records (left). Spatial distribution of the IDEAM meteorological stations (right).

### 2.3 Gridded meteorological datasets

A distinction in two groups can be made regarding gridded datasets for temperature and precipitation: (I) datasets based on observations solely (ground-observed, remotely sensed, or a mixture of these), and (II) datasets based on reanalysis. In this section an overview of the available gridded datasets is provided, and strengths and weaknesses of the different products are highlighted and compared. A selection of products to be used is made based on well-defined selection criteria. Only datasets covering the complete Magdalena basin are considered in this analysis. A tabular overview of all evaluated datasets and their key characteristics is provided in Table 1.

<sup>1</sup> In the final stage of the project, after the climate data analysis and downscaling was performed by FutureWater and the hydrological model of Deltares was calibrated and run using that data, IDEAM meteorological station data was made available to the consortium. The station data was tested as input of the gridded 0.02° hydrological model and it appeared to result in improved temporal patterns for river discharge. Although the downscaled data did show good climate statistics, it was derived from larger spatial scale data and, as expected, appeared to be not as accurate input for the small scale hydrological modelling. As per Deltares' request, the received IDEAM station data was quickly processed using similar downscaling and transformation methods as are described in this report to use in further analyses. Due to time constraints, however, the base and future climate trends and statistics of the IDEAM data could not be analysed and visualised.



Table 1. Gridded meteorological data products available for the Magdalena basin.

Dataset	Type	Coverage	Resolution	Freq.	Period	Parameters	Institute	Free
NCEP/NCAR reanalysis data	Re-analysis	Global	~209 km (T62 grid)	6 hourly	1948 - present	Prec, Tmax, Tmin, Tavg (+ many more)	NCEP/NCAR	YES
CFSR	Re-analysis	Global	~ 50 km (0.5 degree)	1 hourly, 6 hourly, monthly	1979-2010	Prec, Tmax, Tmin, Tavg (+ many more)	NCEP	YES
ERA 15	Re-analysis	Global	basic: ~ 250 km (2.5 degrees) ~ 120 km (N80 grid)	monthly	1979 - 1994	Prec, Tmax, Tmin, Tavg (+ many more)	ECMWF	YES NO
ERA 40	Re-analysis	Global	~ 250 km (2.5 degrees) ~ 120 km (N80 grid)	6 hourly	1957 - 2002	Prec, Tmax, Tmin, Tavg (+ many more)	ECMWF	YES NO
ERA Interim	Re-analysis	Global	~ 70 km (N128 grid)	6 hourly	1979 - present	Prec, Tmax, Tmin, Tavg (+ many more)	ECMWF	YES
ERA 20 CM	Ensemble of climate model integrations	Global	~ 120 km (N80 grid)	3 hourly	1900-2009	Prec, Tavg	ECMWF	YES
NASA MERRA	Re-analysis	Global	~ 70 km (0.5 x 0.67 degrees))	3 hourly	1979 - present	Prec, Tmax, Tmin, Tavg (+ many more)	NASA	YES
Global Meteorological Forcing Dataset for land surface modeling	Re-analysis + observations	Global	~ 50 km (0.5 degree)	3 hourly	1948 - 2008	Prec, Tmax, Tmin, Tavg (+ many more)	Princeton University	YES
CRU TS 3.10.01	Observations	Global	~ 50 km (0.5 degree)	Monthly	1901-2009	cloud cover, DTR, frost days, precipitation, daily minimum temperature, daily mean temperature, daily maximum temperature, vapour pressure, wet days, ETpot	Climate Research Unit at the University of East Anglia	YES
GPPC	Observations	Global	~ 50 km (0.5 degree)	Monthly	1901-2007	Precipitation	Global Precipitation Climatology Centre	YES
GPCP	Observations	Global	~ 250 km (2.5 degrees)	Monthly	1979 - present	Precipitation	GEWEX	YES
CPC-UGBAGDP	Observations	Global	~ 50 km (0.5 degree)	Daily	1979-present	Prec	CPC	YES
DEL	Observations	Global	~ 50 km (0.5 degree)	monthly	1900-2008	Prec, Tair	CCR Univ. Delaware	YES



### 2.3.1 Gridded datasets based solely on observations

#### 2.3.1.1 CRU TS 3.10.01

The CRU dataset can be considered as the oldest and most widely-used gridded meteorological dataset. The first version of the CRU dataset was released in 2000 by the Climate Research Unit at the University of East Anglia (New et al., 1999, 2000), while the latest version was released in 2013 (Harris et al., 2013). The CRU Global Climate Dataset, consists of a multivariate  $0.5^\circ$  by  $0.5^\circ$  resolution mean monthly climatology for global land areas, excluding Antarctica. Together with a mean climatology, which is strictly constrained to the period 1961–1990, there is a monthly time series at the same resolution for the period 1901–2000. The mean 1961–1990 climatology comprises a suite of eleven surface variables, including precipitation, mean, maximum and minimum temperature. Fields of monthly climate anomalies, relative to the 1961–90 mean, were interpolated from surface climate data. The anomaly grids were then combined with a 1961–90 mean monthly climatology to arrive at grids of monthly climate over the 1901–2009 period.

#### 2.3.1.2 GPCP

The Global Precipitation Climatology Project (GPCP) released the version 1 Combined Precipitation Dataset in 1997 (Huffman et al., 1997), while version 2 was released in 2003 (Adler et al., 2003). The product is a global, monthly precipitation dataset covering the period 1979 through 2003. The primary product in the dataset is a merged analysis incorporating precipitation estimates from low-orbit-satellite microwave data, geosynchronous-orbit-satellite infrared data, and rain gauge observations. The dataset is extended back into the pre-microwave era (before mid-1987) by using infrared-only observations calibrated to the microwave-based analysis of the later years. The combined satellite-based product is adjusted by the rain gauge analysis.

#### 2.3.1.3 GPCC

The precipitation dataset developed by the Global Precipitation Climatology Centre (GPCC) was firstly constructed in 1989 and the latest version was published in 2013 (Schneider et al., 2013).. The GPCC has calculated a precipitation climatology for the global land areas for the target period 1951– 2000 by objective analysis of climatological normals of about 67,200 rain gauge stations from its database. GPCC actually published four gridded products, i.e. the Climatology (CLIM) V2011, the Full Data Reanalysis (FD) V6, the Monitoring Product (MP) V4, and the First Guess Product (FG); all publicly available. Depending on the product, four ( $0.25^\circ$ ,  $0.5^\circ$ ,  $1.0^\circ$ ,  $2.5^\circ$  for CLIM), three ( $0.5^\circ$ ,  $1.0^\circ$ ,  $2.5^\circ$ , for FD), two ( $1.0^\circ$ ,  $2.5^\circ$  for MP) or one ( $1.0^\circ$  for FG) resolution is provided.

The FG product is a global gridded product of the monthly precipitation, provided on  $1.0^\circ$  resolution, based on interpolated precipitation anomalies from more than 6000 stations worldwide and is available in near real time. The MP is available within two months after the observation period at  $2.5^\circ$  and  $1.0^\circ$  resolution. This is the oldest GPCC product that went operational in 1986 and has continuously been updated every month since then. Major sample application of the FD product is the verification of reanalysis products like the ERA-Interim reanalysis. It uses the same stations applied to calculate the GPCC Climatology product, i.e. more than 67 200 stations for Version 6. Grid resolutions are  $0.5^\circ$ ,  $1.0^\circ$  and  $2.5^\circ$ . The QC is extended by an additional manual control. Upon substantial improvements of the database, a new version of this product is released, which happens approximately every 1–3 yr.



#### 2.3.1.4 CPC-UGBAGDP

The Unified Gauge-Based Analysis of Global Daily Precipitation (UGBAGDP) dataset has two components: (a) the "retrospective version" which uses 30,000 stations and spans 1979-2005 and (b) the "real-time version" which uses 17,000 stations and spans 2006-present. The daily analysis is constructed on a 0.125° grid over the entire global land areas, and released on a 0.5° grid over the global domain for a period from 1979 (Xie et al., 2007).

#### 2.3.1.5 DEL

The University of Delaware has put data together from a large number of stations, both from the GHCN2 (Global Historical Climate Network) and, more extensively, from the archive of Legates & Willmott (Willmott and Rowe, 1985). The result is a monthly climatology of precipitation and air temperature, both at the surface, and a time series, spanning 1900 to 2010, of monthly mean surface air temperatures, and monthly total precipitation. It is land-only in coverage.

### 2.3.2 Gridded reanalysis datasets

The general purpose of conducting reanalyses is to produce multiyear global state-of-the-art gridded representations of atmospheric states, generated by a constant model and a constant data assimilation system. To use the same model and data assimilation over a very long period was the great advance during the 1990s, because gridded datasets available before 1995 had been created in real time by ever-changing models and analysis methods, even by hand analyses prior to about 1965. The hope was that a reanalysis, made after real time, would help in advancing climate studies by eliminating fictitious trends caused by model and data assimilation changes in real time (Saha et al., 2010).

Global and regional atmospheric retrospective analysis models (reanalyses) play a crucial role in today's hydrological and hydrometeorological research. These global atmospheric reanalyses aim at assimilating a large amount of historical observation data to provide a physically consistent basis for the most important hydrological, hydrometeorological, and atmospheric quantities. To bring these various observations into a consistent scheme, computation of the reanalysis models is performed via state-of-the-art data assimilation methods like three- or four dimensional variational data assimilation (3DVAR or 4DVAR) that constrain the observations with physically reasonable time evolution and budget equations. These reanalyses can be used to analyze the global climate system, atmosphere, and land surface processes on large to continental scales and to understand exchange processes between these different regimes. Global atmospheric reanalyses also are often used as forcing data for regional hydrological or hydrometeorological simulations, such as numerical weather predictions and regional climate simulations (Lorenz and Kunstmann, 2012).

Development of reanalysis<sup>1</sup> datasets has been rapidly increased over the last years. The need of these datasets has mobilized a lot of researchers, and many products can be freely obtained over the Internet. Important to realize is that the core of these datasets are still observations. In cases where data are lacking, in time or space, intelligent data assimilation techniques, based on models and geostatistical analysis, are used to fill these gaps.

Key strengths of reanalysis data are (NCAR, 2013):

---

<sup>1</sup> Reanalysis is a systematic approach to produce data sets for climate monitoring and research. Reanalyses are created via a data assimilation scheme and model(s) which ingest all available observations every 6-12 hours over the period being analysed. Currently, approximately 7-9 million global observations are ingested at each time step (NCAR, 2013).



- Global data sets, consistent spatial and temporal resolution over 3 or more decades, hundreds of variables available; model resolution and biases have steadily improved.
- Reanalyses incorporate millions of observations into a stable data assimilation system that would be nearly impossible for an individual to collect and analyze separately, enabling a number of climate processes to be studied.

Despite these strengths some known weaknesses of reanalysis data should be considered (NCAR, 2013):

- Reanalysis data sets should not be equated with "observations" or "reality".
- The changing mix of observations, and biases in observations and models, can introduce spurious variability and trends into reanalysis output.

Observational constraints, and therefore reanalysis reliability, can considerably vary depending on the location, time period, and variable considered.

#### 2.3.2.1 NCEP/NCAR Reanalysis 1

The NCEP/NCAR reanalysis 1 was published in 1996 (Kalnay et al., 1996). This product is a first generation reanalysis. It uses a frozen global data assimilation system (as of 11 January 1995), which is quite outdated nowadays. Originally planned to span 1957-96 ("40-Year Reanalysis Project"), it was extended back to 1948 and continues to this day. It is used in many publications, making it a useful baseline reference for many computations.

#### 2.3.2.2 NCEP-DOE Reanalysis 2

NCEP-DOE Reanalysis 2 (Kanamitsu et al., 2002) is an improved version of the NCEP-NCAR Reanalysis 1. The improvements include an updated model, better physical parameterizations and assorted error fixes. However, it is still a first generation product.

#### 2.3.2.3 NCEP-CFSR

The NCEP Climate Forecast System Reanalysis (Saha et al., 2010) is the third generation successor of the NCEP/NCAR Reanalysis 1 and 2 (Section 2.3.2.1 and 2.3.2.2). Compared to Reanalysis 1 and 2, CFSR has improved routines and higher spatial resolution. The product covers 1979 to 2010.

Key Strengths (NCAR, 2013):

- Superior to previous NCEP reanalyses with respect to: improved model, finer resolution, advanced assimilation schemes, atmosphere-land-ocean-sea ice coupling, assimilates satellite radiances rather than retrievals
- Accounts for changing CO<sub>2</sub> and other trace gasses, aerosols, and solar variations
- Approaches the horizontal resolution of regional reanalyses like the NARR and Arctic System Reanalysis

Key Limitations (NCAR, 2013):

- Relatively few evaluations of CFSR have been conducted so the performance is not well-known

#### 2.3.2.4 ERA 15

The ERA-15 production system generated re-analyses for 15 years (1979-1993) using a special version of their 1995 operational data assimilation system and model. The resulting analyses



include full model resolution analyses or reduced resolution analyses and climate and statistics data. ERA-15 is the precursor to ERA-40 and ERA-Interim. It is recommended that the ERA-Interim products be used rather than the ERA-15 or ERA-40 (NCAR, 2013). Key Limitations (NCAR, 2013):

- Excessive tropical precipitation.
- Hydrologic budget was not 'closed'.
- Also there was an incorrect southward shift in the ITCZ over Africa in 1987 most likely due to the assimilation and bias correction of satellite data

#### 2.3.2.5 ERA 40

ERA 40 is a second generation reanalysis (Uppala et al., 2005). It is the first reanalysis to directly assimilate satellite radiance data (TOVS, SSM/I, ERS and ATOVS). Cloud Motion Winds are also used. The result is better circulation over the tropics and southern hemisphere.

Key Strengths (NCAR, 2013):

- Assimilates satellite radiances directly (TOVS, SSM/I, ERS and ATOVS data).
- Cloud Motion Winds will be used from 1979 onwards.

Key Limitations (NCAR, 2013):

- Tropical moisture (precipitation, total column water vapor) larger than observed from 1991 onward
- Precipitation greatly exceeds evaporation
- Brewer Dobson circulation is too intense; Spurious Arctic temperature trends

#### 2.3.2.6 ERA Interim

Using a much improved atmospheric model and assimilation system from those used in ERA-40, ERA-Interim represents a third generation reanalysis (Dee et al., 2011). Several of the inaccuracies exhibited by ERA-40 such as too-strong precipitation over oceans from the early 1990's onwards and a too-strong Brewer-Dobson circulation in the stratosphere, were eliminated or significantly reduced. ERA-Interim now extends back to 1979 and the analysis continues to be extended forward in near-real-time.

Key Strengths (NCAR, 2013):

- Spatially and temporally complete data set of multiple variables at high spatial and temporal resolution
- Improved low-frequency variability (compared to ERA-40)
- Improved stratospheric circulation (compared to ERA-40)

Key Limitations (NCAR, 2013):

- Too intense of a water cycling (precipitation, evaporation) over the oceans
- In the Arctic: positive biases in temperature and humidity below 850hPA compared to radiosondes; does not capture low-level inversions

#### 2.3.2.7 NASA MERRA

The Modern Era Retrospective-Analysis for Research and Applications (MERRA) (Rienecker et al., 2011) was undertaken by NASA's Global Modeling and Assimilation Office with two primary



objectives: to place observations from NASA's Earth Observing System satellites into a climate context and to improve upon the hydrologic cycle represented in earlier generations of reanalyses. MERRA was generated with version 5.2.0 of the Goddard Earth Observing System (GEOS) atmospheric model and data assimilation system (DAS), and covers the modern satellite era from 1979 to the present. Specifically, the GEOS-DAS Version 5 implements Incremental Analysis Updates (IAU) to slowly adjust the model states toward the observed state. MERRA is a 3rd generation reanalysis product (NCAR, 2013).

Key Strengths (NCAR, 2013):

- Significant improvement in precipitation and water vapor climatology over older reanalyses
- The IAU procedure in which the analysis correction is applied to the forecast model gradually ameliorates precipitation spin-down during early stages of the forecast, and allows for higher frequency output including selected hourly fields
- Provides vertical integrals and analysis increment fields for the closure of atmospheric budgets

Key Limitations (NCAR, 2013):

- Changes in the observing system strongly affect trends in many fields (as for other reanalyses); for example P-E exhibits spurious increases associated with assimilating radiances from the AMSU starting in 1998 and to a lesser extent, SSM/I in 1987
- Spatial discontinuity in central African moisture fields associated with rawinsonde input
- The assimilation routine is "frozen" and will not be updated for newer satellite instruments, so quality will eventually degrade as current instruments expire

#### 2.3.2.8 NOAA 20CR v2

The Twentieth Century Reanalysis (20CR) developed by the National Oceanic and Atmospheric Administration (NOAA), provides a comprehensive global atmospheric circulation data set spanning 1870-2010 (Compo et al., 2011). It assimilates only surface pressure reports and uses observed monthly sea-surface temperature and sea-ice distributions as boundary conditions. Its chief motivation is to provide an observational validation data set, with quantified uncertainties, for assessing climate model simulations of the 20th century, with emphasis on the statistics of daily weather. The analyses are generated by assimilating only surface pressures and using monthly SST and sea ice distributions as boundary conditions within a 'deterministic' Ensemble Kalman Filter (EKF). A unique feature of the 20CR is that estimates of uncertainty are derived using a 56 member ensemble. Overall, the quality is approximately that of current three-day NWP forecasts.

Key Strengths (NCAR, 2013):

- Length of record
- Estimates of uncertainty

Key Limitations (NCAR, 2013):

- As with all reanalyses, users should take care in interpreting long-term trends - inconsistencies between 20CR and other data have been reported



### 2.3.3 Other products

#### 2.3.3.1 Princeton Global Meteorological Forcing Dataset for land surface modeling

The Princeton Global Meteorological Forcing Dataset for land surface modeling (hereafter called PRINCETON) provides near-surface meteorological data for driving land surface models and other terrestrial modeling systems (Sheffield et al., 2006). The dataset is constructed by combining a suite of global observation-based datasets with the National Centers for Environmental Prediction–National Center for Atmospheric Research (NCEP–NCAR) reanalysis. Known biases in the reanalysis precipitation and near-surface meteorology have been shown to exert an erroneous effect on modeled land surface water and energy budgets and are thus corrected using observation-based datasets of precipitation, air temperature, and radiation.

Corrections are also made to the rain day statistics of the reanalysis precipitation, which have been found to exhibit a spurious wavelike pattern in high-latitude wintertime. Wind-induced under catch of solid precipitation is removed using the results from the World Meteorological Organization (WMO) Solid Precipitation Measurement Intercomparison. Precipitation is disaggregated in space to 1.0° by statistical downscaling using relationships developed with the Global Precipitation Climatology Project (GPCP) daily product. Disaggregation in time from daily to 3 hourly is accomplished similarly, using the Tropical Rainfall Measuring Mission (TRMM) 3-hourly real-time dataset. Other meteorological variables (downward short- and longwave radiation, specific humidity, surface air pressure, and wind speed) are downscaled in space while accounting for changes in elevation.

The dataset is currently available at 0.5 degree, 3-hourly resolution globally for 1948-2008.

#### 2.3.3.2 ERA-CLIM reanalysis products

ECMWF is currently developing the next generation of reanalysis products. One of them (ERA-20CM) was recently released. The ERA-20CM is an ensemble of ten model integrations for 1900-2009. The spatial resolution is 125 x 125 km. Sea-surface temperature and sea-ice cover are prescribed by an ensemble of realizations (HadISST2), as recently produced by the Met Office Hadley Centre within ERA-CLIM. Variation in these realizations reflects uncertainties in the available observational sources on which this product is based.

Forcing terms in the model radiation scheme follow CMIP5 recommendations, without variations, i.e. any effect on their uncertainty is neglected. These include solar forcing, greenhouse gases, ozone and aerosols. Both the ocean-surface and radiative forcing incorporate a proper long-term evolution of climate trends in the 20th century, and the occurrence of major events, such as the El Nino-Southern Oscillations and volcanic eruptions. No atmospheric observations were assimilated. For this reason ERA-20CM is not able to represent actual synoptic situations. The ensemble should, however, be able to provide a statistical estimate of the climate. This is indeed confirmed. Overall, the temperature rise over land is in fair agreement with the CRUTEM4 data set. Over the last two decades the warming over land exceeds the warming over sea, which is consistent with models from the Intergovernmental Panel on Climate Change (IPCC), as well with the currently state-of-the-art ECMWF reanalysis (ERA-Interim) (Peubey et al., 2013).

Other products that will be released by ERA in the framework of the ERA-CLIM project are ERA-20C (end 2013), ERA-20CL (end 2013) and ERA-SAT (2015) (Dee, 2013). ERA-20C is a reanalysis of surface pressure variables based on a revised version of the ERA-20CM model and forcings. ERA-20CL is for the land surface only and is forced by ERA-20C. ERA-SAT is a



new reanalysis of the satellite era to replace ERA-Interim and will have a 40x40 km spatial resolution.

## 2.4 Selection of a dataset

A homogenous and detailed climate data set is required for calibration of the hydrological model and as a reference dataset for the downscaling of future GCM climate scenarios. Because of the sparse, incomplete and unobtainable meteorological in situ records in the Magdalena basin, interpolation of a high quality and high resolution gridded dataset is preferred at this time.

A previous study has selected a number of gridded datasets, both solely based on observations and based on reanalysis, and evaluated their usability and quality based on a number of selection criteria (Lutz et al., 2014). The selection criteria that were used are the following:

- Based on proven (state of the art reanalysis) techniques
- High spatial resolution
- High temporal resolution
- Good consistency with ground-observations
- Closing water balances
- Suitable for tropical areas
- Well documented

Lutz et al. (2014) found that the gridded datasets based solely on observations generally performed worse than the reanalysis-based sets. An overview of the final scores of the both type of datasets are shown in



Table 2 and Table 3. The tables show that ERA Interim has the highest score closely followed in rank by NASA MERRA and PRINCETON. However, as the ERA Interim dataset potentially has a too intense water cycling (precipitation, evaporation) over the oceans and the Magdalena basin climate is highly affected by atmospheric conditions over the Pacific Ocean it is chosen to discard this dataset for reliable use this area.

The lack of in situ observation data in the Magdalena basin that can be used for bias correction of a gridded dataset provides PRINCETON with a slight advantage over NASA MERRA. Namely, PRINCETON shows a better agreement with observation data due to the pre-applied bias correction and has better accessibility and documentation. This dataset is therefore chosen to downscale for the hydrological modelling of the Magdalena basin. As the Princeton dataset is only available up to 2008, the 30 year period 1979-2008 is chosen as reference period, which is assumed to be climatically equal to the 1981-2010 period.



Table 2. Scores for selection criteria for observation-based products.

Dataset	Type	Parameters	Spatial resolution	Temporal resolution	Temporal coverage	Suitable for tropical areas	Established in scientific literature	Documentation/Accessibility	Score
CRU TS 3.10.01	Observations	Prec, Tmax, Tmin, Tavg	3	1	3	2	3	3	15
GPCC	Observations	Prec	3	1	3	2	3	3	15
GPCP	Observations	Prec	1	1	1	2	2	3	10
CPC-UGBAGDP	Observations	Prec	3	3	1	2	2	2	13
DEL	Observations	Prec, Tavg	3	1	3	2	2	1	12

Table 3. Scores for selection criteria for reanalysis products (Lutz et al., 2014).

Dataset	Type	Parameters	State-of-the-art	Spatial resolution	Temporal resolution	Suitable for tropical areas	Established in scientific literature	Consistent with ground observations	Closing water balance	Documentation/Accessibility	Score
NCEP/NCAR reanalysis	Re-analysis	Prec, Tmax, Tmin, Tavg	1	1	3	2	3	2	1	3	<b>16</b>
CFRSR	Re-analysis	Prec, Tmax, Tmin, Tavg	3	3	3	2	1	2	2	2	<b>18</b>
ERA 15 basic	Re-analysis	Prec, Tmax, Tmin, Tavg	1	1	1	3	3	2	1	3	<b>15</b>
ERA 15 advanced			1	2	1	3	3	2	1	1	<b>14</b>
ERA 40 basic	Re-analysis	Prec, Tmax, Tmin, Tavg	2	1	3	3	3	2	2	3	<b>19</b>
ERA 40 advanced		Prec, Tmax, Tmin, Tavg	2	2	3	3	3	2	2	1	<b>18</b>
ERA Interim	Re-analysis	Prec, Tmax, Tmin, Tavg	3	3	3	3	2	3	3	3	<b>23</b>
ERA 20 CM	Ensemble of climate model integrations	Prec, Tavg	3	2	3	3	1	1	2	1	<b>16</b>
NASA MERRA	Re-analysis	Prec, Tmax, Tmin, Tavg	3	3	3	2	2	2	2	3	<b>20</b>
PRINCETON	Re-analysis + observation	Prec, Tmax, Tmin, Tavg	2	3	3	2	2	3	3	3	<b>21</b>



## 2.5 Downscaling of gridded data to modelling scale

To be able to use the 0.5° PRINCETON data as input of the hydrological model it is downscaled to the 0.02° modelling grid that was defined for the Magdalena basin by Deltares. A comparison of the two grids and a GCM grid are shown in Figure 3. The daily precipitation data is interpolated using a bilinear interpolation algorithm and is subsequently converted from units in  $\text{kg m}^{-2} \text{s}^{-1}$  to  $\text{mm d}^{-1}$ .

The temperature data, after a similar bilinear interpolation procedure, undergoes a simple lapse rate correction that is based on SRTM elevation data using:

$$T_{i,j,k}^{\text{corr}} = T_{i,j,k}^{\text{int}} - h \quad (1)$$

where  $T_{i,j,k}^{\text{corr}}$  is the lapse corrected temperature,  $T_{i,j,k}^{\text{int}}$  the interpolated PRINCETON temperature at the earth's surface,  $h$  the lapse rate of  $0.0065 \text{ } ^\circ\text{C m}^{-1}$  and  $h$  the difference between the mean elevation of the encompassing PRINCETON 0.5° cell and the elevation of cell  $i,j$ .

The hydrological model also requires the input of a daily set of reference evapotranspiration data ( $ET_0$ ). Because both in situ measurements and gridded (reanalysed) data of this climatic variable are unavailable they are estimated from the  $T_{\min}$  and  $T_{\max}$  variables that are available in the PRINCETON dataset using a modified Hargreaves equation (Droogers and Allen, 2002):

$$ET_0 = 0.0025 + 0.408RA \frac{(T_{\min} + T_{\max})}{2} - 16.8 (T_{\max} - T_{\min})^{0.5} \quad (2)$$

where  $RA$  is extraterrestrial radiation in  $\text{MJ m}^{-2} \text{d}^{-1}$ , which is determined for each PRINCETON grid cell and each day of the year using the methods of Duffie & Beckman (1991). Examples of the downscaled reference climate data are shown in Figure 4.

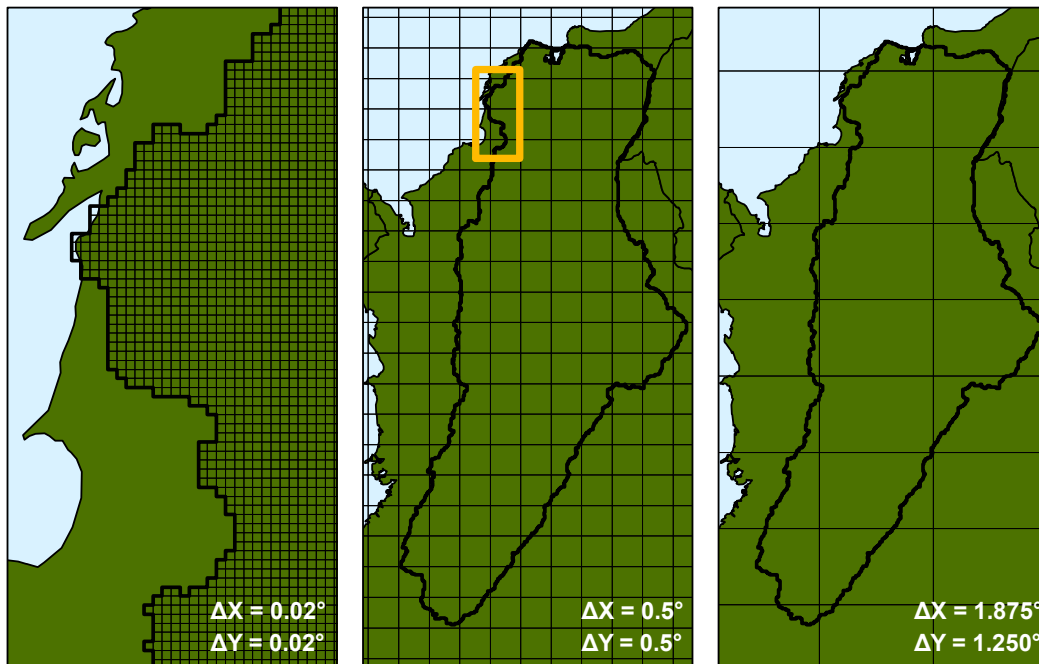


Figure 3. The three different grid scales used in this project. The hydrological model grid (left), the PRINCETON data grid (center) and an example of a GCM grid (right).

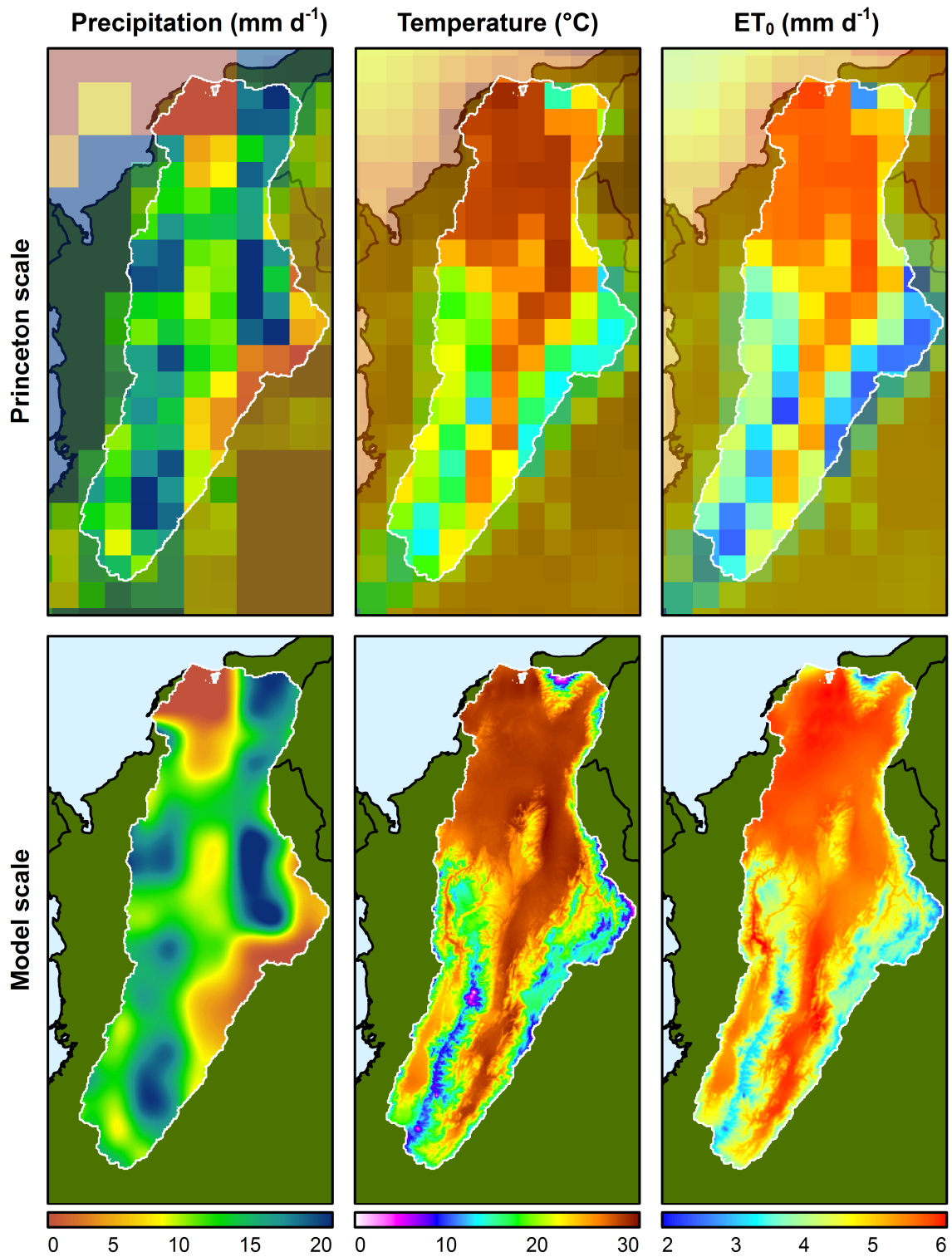


Figure 4. Examples of a time step of the original PRINCETON precipitation and temperature data as well as the temperature-derived reference evapotranspiration (top row). The same time step as downsampled and clipped to the  $0.02^{\circ}$  hydrological model grid is shown in the bottom row.



## 3 Future climate data<sup>1</sup>

### 3.1 Introduction

To make an assessment of future flooding risks in the Magdalena basin in the context of the tipping point analyses it is important to understand what changes will occur to all factors that can affect flooding. Besides political, societal and economic aspects, future changes in river discharge are of major influence in future flooding frequency and severity. To determine those discharge changes for the Magdalena River and its tributaries it is necessary to use the future climate data output of global climate models (GCMs) as input for hydrological modelling. They are simply the only source of future climate data. Important to note, however, is that the GCMs are mere models and drawing conclusions using their outputs must be done with care.

#### 3.1.1 Interpolation of global climate model data

Although one could downscale GCM data directly to the hydrological model scale this would lead to inaccurate results for two main reasons. First of all, the GCM spatial scale is substantially different (Figure 3). Orographic and topographic features as well as presence of large water bodies, all very distinct in and near the Magdalena basin (Figure 1), are incorporated in the GCMs on a significantly different scale than in the hydrological model. As a result direct interpolation to the 0.02° modelling grid would not give an accurate representation of their influence due to significant smoothing and generalization. Secondly, using different types of datasets for calibration and future input will likely yield inaccurate results of the hydrological model as the datasets can have considerably different day to day variation of its climate variables.

#### 3.1.2 Transformation of historical series

A solution is to combine GCM information with a reference meteorological time series. Statistics of a GCM control and future climate can be used to scale the values of the reference series so that they can be taken as representative for the future climate. This way the GCM signal is incorporated into the high spatial scale reference data that is more suitable for hydrological modelling. In this method the chosen GCM control climate period must be climatically equal to the period of the historical series. The future period can be chosen freely, although it should be of a similar length. This statistical scaling is called a delta change method.

For precipitation the classic delta change method comprises a linear transformation of the reference time series using differences between control and future means, which can result in an unrealistic change of the precipitation distribution compared to the changes that occur in GCMs. Detailed insight in the change of the extremes in the precipitation distribution is valuable for research and modelling, as many environmental processes trigger only at extreme precipitation amounts. This is, of course, also very true for flooding. To accommodate this, a revised version of the delta change method was developed (Van Pelt et al., 2012) called the advanced delta change (ADC) method.

---

<sup>1</sup> Parts of this chapter were largely taken from a previous report on the ADC method and CMIP5 GCMS from the author (Kraaijenbrink, 2013). This report was written while employed at the Royal Netherlands Meteorological Institute (KNMI) and it is publically available from their website.



The revised method focuses primarily on increasing the detail in the high end of the precipitation distribution as it is aimed at improving modelling of extreme discharge events. The main difference with the original delta change method is that the revised method uses a non-linear transformation that is based on the 60% and 90% quantiles of the precipitation distribution (Figure 6). Furthermore, biases between the quantiles of the control period of the GCM and the observation series are corrected for.

### 3.2 Global climate models

#### 3.2.1 GCMs, CMIP5 and RCPs background

The latest generation of GCMs was developed as part of the Coupled Model Intercomparison Project Phase 5 (CMIP5), which aims to provide sets of future climate data by coordinating many institutions to perform climate model experiments (PCMDI, 2014). With this phase of the project a new method of climate forcing using representative concentration pathways (RCPs) is introduced in the models (Taylor et al., 2012). The new approach is to not directly prescribe certain greenhouse gas emission scenarios as drivers as was the case before, but a predetermined future path of radiative forcing in  $W/m^2$  by using the RCPs (Figure 5). However, the paths were determined with certain scenarios in mind (IIASA, 2013).

There are four main RCPs defined up to the year 2100, each developed by an independent research group using integrated assessment analysis and modelling. Temporal extensions to the year 2300 are made using simple algorithms to drive long-term earth-system simulation experiments. The RCPs have a suffix that indicates the radiative forcing in  $W/m^2$  by the year 2100 as reported by the modelers (IIASA, 2013).

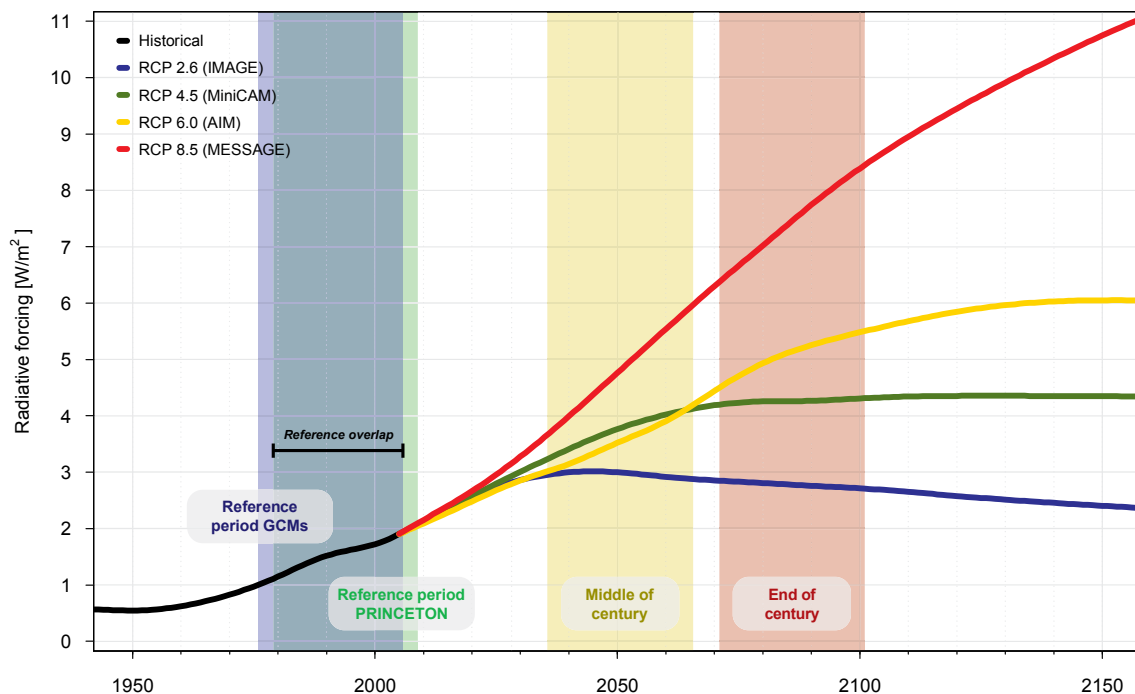


Figure 5. The representative concentration pathways as defined for CMIP5 and the four 30-year climate periods used in this project (after Kraaijenbrink (2013), data from IIASA (2013)).



### 3.2.2 Climate periods of interest

The nature of the downscaling method, i.e. by using a reference series, forces one to look at periods in the future that are of relatively similar length as that series. In the framework of the project it is valuable to gain insight in the future changes of a period that is longer than the 30-year climate period of the reference series. For this reason it is chosen to look at two separate future 30-year climate periods that are commonly used in climate research (Figure 5): middle of century (MOC), 2036-2065; end of century (EOC), 2071-2100.

The project aims at using a reference series that is as recent as possible, which for the PRINCETON data is up to 2008. The control runs of the CMIP5 GCM runs, however, only go up to 2005 and therefore the 30-year 1976-2005 period is used as GCM control climate. Is it is most accurate to use exactly the same period for the reference series as for the GCM control series but it is not feasible in this case. The overlap between the two periods is still 27 years (Figure 5), however, and the two periods are therefore assumed to have an equal climate.

### 3.2.3 Selection of GCMs and model realizations

To represent the future climate a total of two realizations are desired from two different GCMs. For each realization two runs are chosen that have a RCP climate forcing of 4.5 and 8.5 W/m<sup>2</sup>. As a large CMIP5 ensemble analysis to select optimal candidates is beyond the scope of this project, it is chosen to evaluate all realizations from two well-known GCMs and select two based on the results. The CMIP5 GCMs that were selected for the analysis are MPI-ESM-LR from Max-Planck Institute for Meteorology and HadGEM2-ES from Met Office that have 3 and 4 realizations available respectively for the selected RCPs (Table 4).

For the analysis, differences between the monthly precipitation distributions of a realization's control and future period were evaluated. The two realizations that span the widest range of changes between the two periods were selected. This way the uncertainty in future climate as expressed by the GCM realizations is best expressed in the final outcomes of the hydrological model. In chapter 3.4 the range of differences between reference and transformed series spanned by all realizations are presented graphically.

Table 4. Examined GCM realizations. The marked realizations are selected for the final transformation of the Magdalena baseline climate data.

GCM	Institute	RCP	Realization
MPI-ESM-LR	Max-Planck Institute for Meteorology Hamburg, Germany	4.5	<i>r1i1p1</i>
			<b>r2i1p1</b>
			<i>r3i1p1</i>
		8.5	<i>r1i1p1</i>
			<b>r2i1p1</b>
			<i>r3i1p1</i>
HadGEM2-ES	Met Office Exeter, United Kingdom	4.5	<b>r1i1p1</b>
			<i>r2i1p1</i>
			<i>r3i1p1</i>
			<i>r4i1p1</i>
		8.5	<b>r1i1p1</b>
			<i>r2i1p1</i>
			<i>r3i1p1</i>
			<i>r4i1p1</i>



### 3.3 Advanced delta change method

As already mentioned in section 3.1.2, the advanced delta change method (Van Pelt et al., 2012) comprises a non-linear transformation of daily observed precipitation series by using a climate signal from a GCM. Both datasets must be on the same spatial scale and therefore a bilinear interpolation of the GCM data to the PRINCETON grid is performed.

The ADC method does not act on the daily values itself, but rather on 5-day precipitation sums. This is performed as extreme discharge events depend on multiple days of extreme precipitation. In practice, the use of 5-day sums results in 73 non-overlapping sums in a 365-day year. For leap years an extra five day sum is introduced that covers 24-29 February. A specific month is assigned to each five day sum, not completely analogous to Gregorian calendar months. Namely, the months January up to November are each assigned to consecutive groups of six 5-day sums while December is assigned to the remaining seven 5-day sums. Figure 7 presents a flowchart that denote all steps of the ADC method that are explained in this section as well as the different temporal scales involved in each step.

For the transformation of the observed 5-day precipitation sums ( $P$ ) two different equations are used, i.e. for precipitation sums that are smaller or larger than their 90% quantile ( $P_{90}$ ). This quantile is determined per calendar month and per common grid cell over the entire reference period; hence there are twelve different  $P_{90}$  values per grid cell.

The two transformation equations are:

$$P^* = aP^b \quad \text{for } P^O < P_{90}^O \quad (3)$$

$$P^* = \overline{E^F} / \overline{E^C} \cdot (P^O - P_{90}^O) + a(P_{90}^O)^b \quad \text{for } P^O > P_{90}^O \quad (4)$$

where  $P^*$  represents the transformed 5-day sums,  $P$  the observation 5-day sums,  $P_{90}$  the 90% quantile and  $a$  and  $b$  are the transformation coefficients. The superscripts  $^O$ ,  $^C$  and  $^F$  denote whether the variable represents respectively the observation time series, the GCM control series or the GCM future series. For 5-day precipitation sums that exceed the  $P_{90}$  of their month an excess value ( $E$ ) is determined, which is the part of the precipitation that is above  $P_{90}$  Figure 6. It is calculated by:

$$E = P - P_{90} \quad (5)$$

The mean future and control excesses in Equation 2 are, similarly to  $P_{90}$ , determined on a monthly basis per grid cell over the entire period by:

$$\overline{E^C} = \frac{\sum P^C - P_{90}^C}{n^C} \quad \text{and} \quad \overline{E^F} = \frac{\sum P^F - P_{90}^F}{n^F} \quad (6)$$

The linear scaling of the transformed precipitation with the ratio of future and control excess in Equation 2 expresses a change in the slope of the extreme value plot of the 5-day maximum precipitation amounts (appendix in van Pelt et al., 2012). It also avoids unrealistically high transformed precipitation values that may occur when Equation 1 is used for  $P > P_{90}$  and  $b > 1$ . The transformation coefficients  $a$  and  $b$  are derived from the 60% and 90% quantiles by:

$$b = \frac{\log\{g_2 \cdot P_{90}^F / (g_1 \cdot P_{60}^F)\}}{\log\{g_2 \cdot P_{90}^C / (g_1 \cdot P_{60}^C)\}} \quad (7)$$



$$a = P_{60}^F / (P_{60}^C)^b \cdot g_1^{1-b} \quad (8)$$

The calculation of the transformation coefficients requires bias correction factors  $g_1$  and  $g_2$  that address systematic differences between the  $P_{60}$  and  $P_{90}$  of the observations and the GCM control series (Figure 6) to ensure a proper reproduction of the relative changes in these quantiles during the transformation. The correction factors are determined by:

$$g_1 = P_{60}^O / P_{60}^C \quad (9)$$

$$g_2 = P_{90}^O / P_{90}^C \quad (10)$$

To reduce sampling variability in the transformation coefficients, the  $P_{60}$  and  $P_{90}$  are smoothed temporally by using a weighted mean with weights of 0.25, 0.5 and 0.25 on respectively the previous, current and next month. The mean excesses ( $\overline{E}^C$  and  $\overline{E}^F$ ) are smoothed temporally in a similar manner.

There is also noise present in the parameters spatially (van Pelt et al., 2012). This is especially an issue for the  $b$  coefficient that has a relatively large influence in the transformation and could cause considerable and unrealistically large differences in transformation results of neighboring common grid cells. Therefore spatial smoothing is applied using a 3x3 moving window operator (Burrough and McDonnell, 1998). The ratio between the control and future mean excesses used in Equation 4 is smoothed spatially as well.

When the 5-day precipitation sums are transformed a change factor can be determined for each sum that is subsequently applied to its corresponding five days of daily observations. The individual days within the five day groups are thereby transformed with an equal change factor. This change factor ( $R$ ) is determined by:

$$R = P^* / P \quad (11)$$

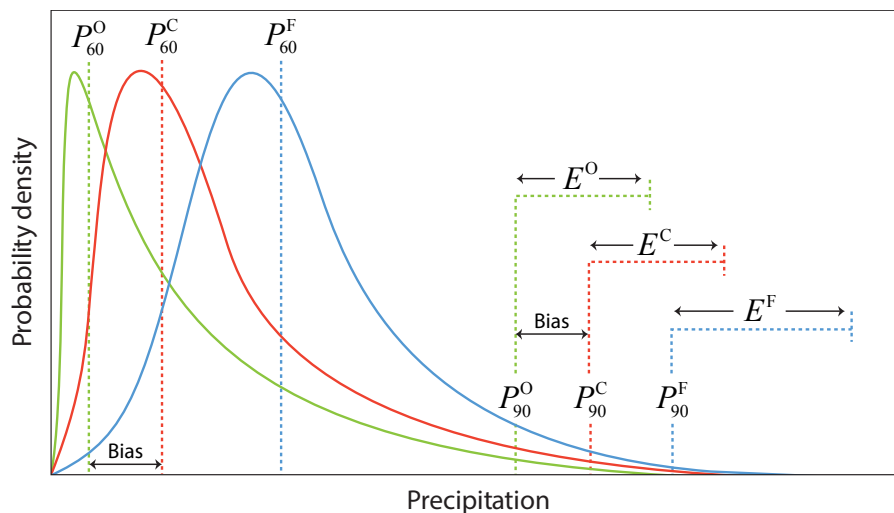


Figure 6. Schematic examples of precipitation distributions and the distribution characteristics used for application of the advanced delta change method (after Kraaijenbrink, 2013).

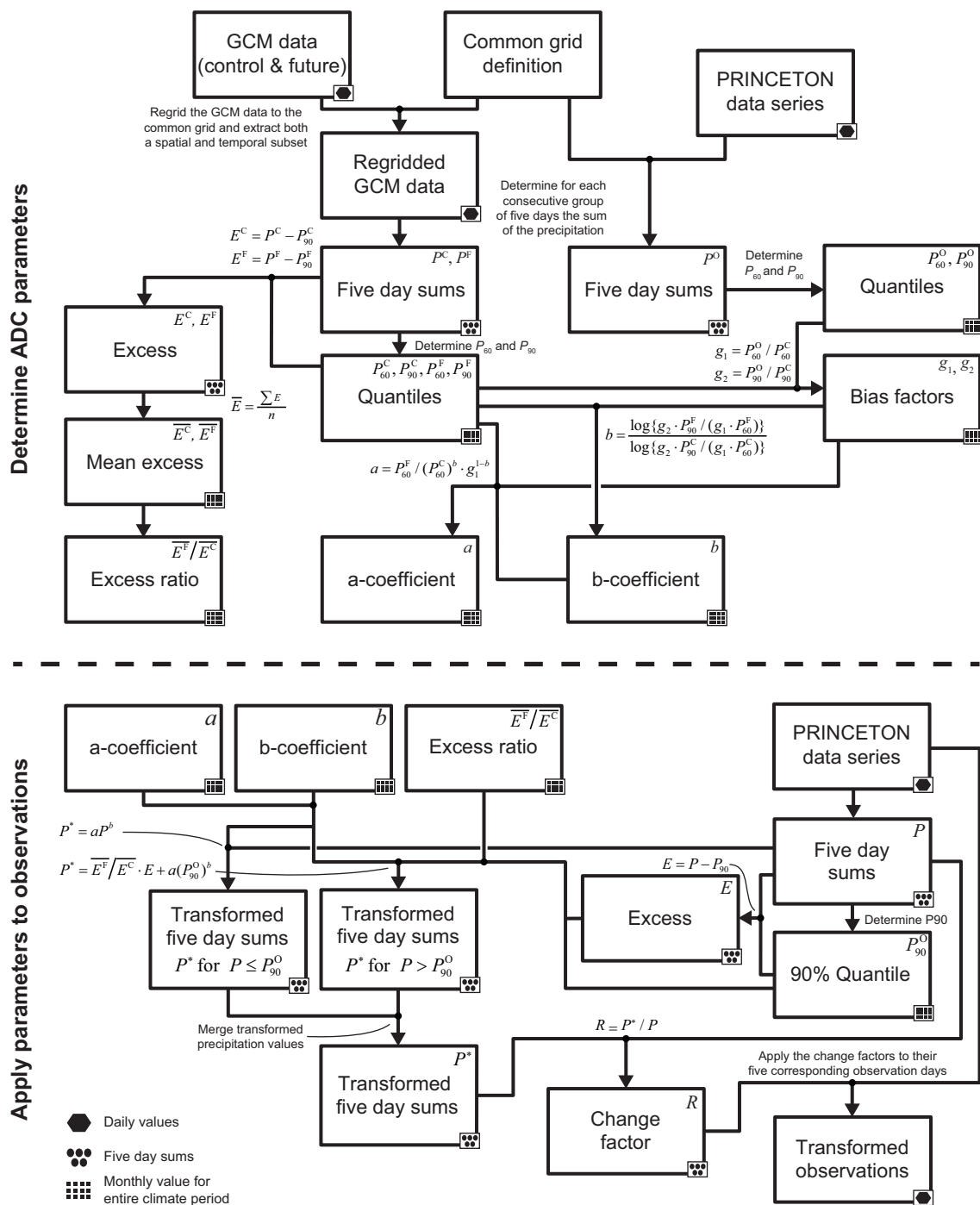


Figure 7. Flowchart overview of the steps performed to apply the advanced delta change method to the PRINCETON reference series (after Kraaijenbrink, 2013).



### 3.4 Temperature transformation

For modelling purposes temperature data is also required. Besides the average temperature, minimum and maximum temperatures are needed to estimate reference evapotranspiration (Equation 2). To accommodate in this need, PRINCETON series for the Magdalena basin ( $T_{\text{avg}}$ ,  $T_{\text{min}}$  and  $T_{\text{max}}$ ) are transformed to values representative for the future by statistical scaling using equivalent GCM variables. The temperature transformation, contrary to that of precipitation, is linear in nature and has the form (van Pelt et al., 2012):

$$T^* = \frac{\sigma^F}{\sigma^C} (T - \overline{T^O}) + \overline{T^O} + \overline{T^F} - \overline{T^C} \quad (12)$$

where  $T^*$  represents the transformed temperature;  $T$  the observed temperature;  $\overline{T^O}$ ,  $\overline{T^C}$  and  $\overline{T^F}$  the monthly mean of respectively the observed, control and future temperature;  $\sigma^C$  and  $\sigma^F$  the standard deviations of the daily control and future temperature calculated per calendar month.

The means and standard deviations are, similarly as for the ADC precipitation transformation, determined on the PRINCETON grid scale and therefore the GCM temperature data is downscaled to the grid using bilinear interpolation. A similar month-based temporal smoothing as for precipitation is applied to the standard deviations. The temperature transformation operates directly on daily values and therefore the transformation does not require the use of a change factor.



## 4 Climate trends

### 4.1 Baseline climate 1979-2008

The state of the climate in the Magdalena basin for 1979-2008 can be constructed using the PRINCETON dataset. The processed PRINCETON series, being a downscaled reanalysis dataset, will likely have small deviations on a day to day scale with the actual situation. However, by focusing on annual, seasonal and monthly climate trends it will provide a good insight in the climate of the basin.

#### 4.1.1 Inter-annual trends

To evaluate the annual trends of precipitation and temperature their daily values were first respectively summed and averaged separately for each year on the grid cell scale. The annual values per grid cell were subsequently spatially averaged to obtain basin-wide values for the climate variables.

##### 4.1.1.1 Annual precipitation

The annual trends found for precipitation over the 1979-2008 period are small (Figure 8). The 30-year precipitation trend comprises a yearly increase of a mere 3.61 mm, which is 0.18% of the 30-year mean of 1898 mm yr<sup>-1</sup>. The results of the computed trend are insignificant, however, as it has a very low goodness of fit due to the broad scatter of only 30 input values. The 5-year moving average does show relatively large short term trends that go up to about 100 mm yr<sup>-1</sup>.

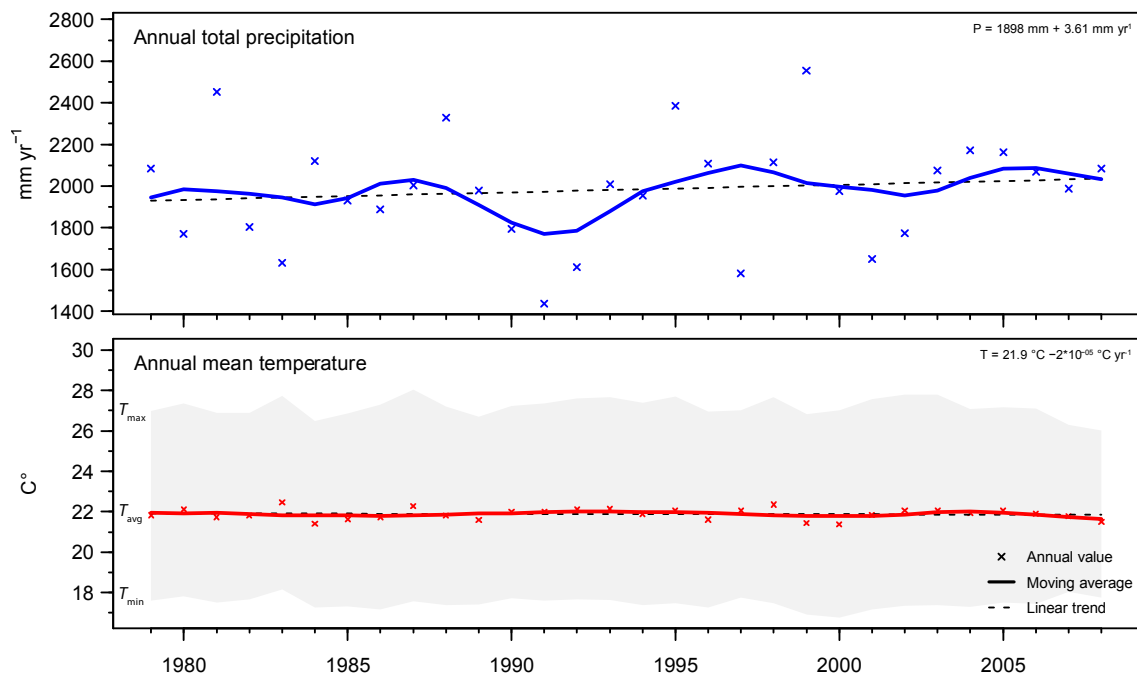


Figure 8. Annual precipitation and mean temperature for the PRINCETON 1979-2008 data series. The calculated annual values are represented by the points and a 5-year moving average by the solid line. The determined 30-year linear trends are shown as dashed line and their parameters are displayed in the upper right.

#### 4.1.1.2 El Niño Southern Oscillation

Large year to year variations in annual precipitation are present for the Magdalena basin (Figure 8). For instance, the year 1997 had about 500 to 600 mm less precipitation than both the preceding and following year. This is about ~30% of the 30-year mean, which is a considerable difference. These strong anomalies are caused by the influence of the El Niño Southern Oscillation (ENSO).

Colombia's climate, due to the country's equatorial location on the west coast of South America, encounters strong influences of the sea surface temperature (SST) of the Pacific Ocean. The large annual differences in SST related to the ENSO's El Niño and La Niña phenomena can cause respectively large negative and positive anomalies in rainfall, river discharges, soil moisture and vegetation conditions. Their effects are phase-locked to the seasonal cycle, being stronger during December–February and weaker during March–May (Poveda et al., 2010; Ward et al., 2014).

The monthly SST anomalies for the central Pacific area (Figure 9), which are an indicator for the phase of the ENSO (NOAA, 2014), show there are clear agreements between the SST anomalies and the precipitation anomalies in the Magdalena basin (Figure 8). Although it is important to study the effects of ocean current and SST anomalies on historical and GCM climate data, especially for a country as Colombia that considerably experiences the effect of the ENSO, the related processes are very intricate and hence beyond the scope of this project's analyses.

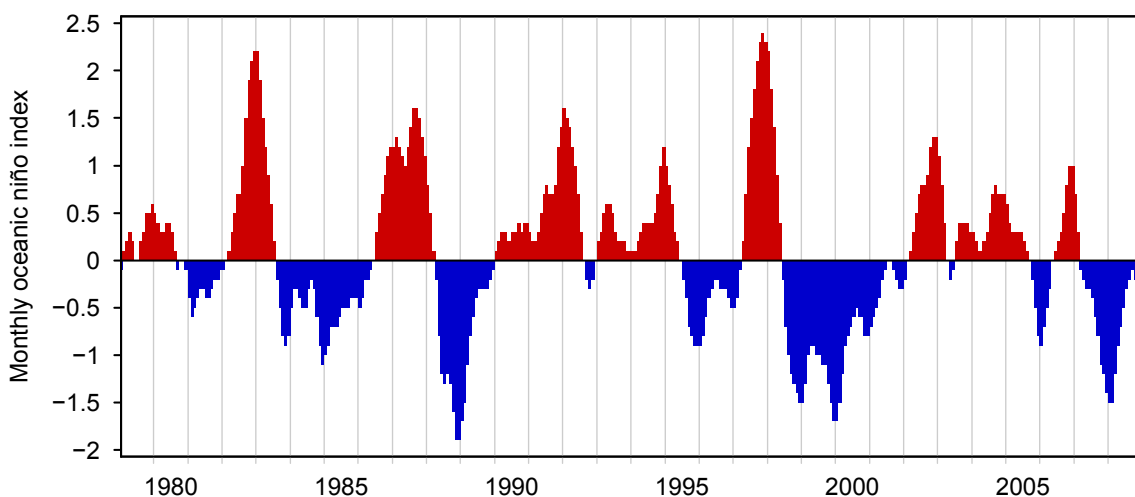


Figure 9. Indicator of the strength of the El Niño Southern Oscillation; the monthly oceanic Niño index. Positive and negative values indicate respectively El Niño and La Niña states. Values in the range -0.5 to 0.5 are considered to be neutral state values [data from NOAA, 2014].

#### 4.1.1.3 Annual temperature

Temperature in the Magdalena basin is very constant. Over the 30-year climate period basin average daily temperature ranges between 18.6 and 25.4 °C with a standard deviation of only 0.74 and a mean of 21.8 °C. The annual mean temperatures are also very constant (Figure 8). The linear trend computed for the entire period is a yearly decrease of 0.00002 °C, which is of course insignificantly small. Reference evapotranspiration has similar annual invariabilities as temperature, as for this project it is directly obtained from  $T_{\min}$  and  $T_{\max}$  using a modified Hargreaves method (Equation 2).



## 4.1.2 Intra-annual trends

### 4.1.2.1 Precipitation

To visualize the monthly variation of precipitation in the Magdalena basin boxplots are made that show the distribution of daily basin average precipitation values for the entire 30-year period grouped per calendar month (Figure 10). Clearly noticeable are the two precipitation peaks at April-May and Oct-Nov. These rain seasons that have large amounts of precipitation are related to the warm and humid convective air near the intertropical convergence zone (ITCZ) that forms large clouds. Colombia's location is right in between the two local settings of the ITCZ, i.e. it is located in just north of Colombia in July and in the south of Colombia in January. Therefore the ITCZ and its rains traverse the country twice a year.

Although both peaks are fairly similar in precipitation distributions, the Oct-Nov precipitation increase is slightly more pronounced. Interestingly, the period in between the rain seasons has overall considerably less precipitation but does have outliers that are of a similar scale. In terms of evaluating future flooding risk this reinforces the fact that it is important to estimate how precipitation distributions will change during the rain seasons and in between. The December-February period is clearly the period with the least precipitation in the basin.

Beside the considerable increase in precipitation during the rain seasons the variation increases as well, noticeable by the increased height of the boxes and whiskers, i.e. the interquartile range. This too can be ascribed to the ITCZ, as the related torrential rains are generally quite erratic temporally.

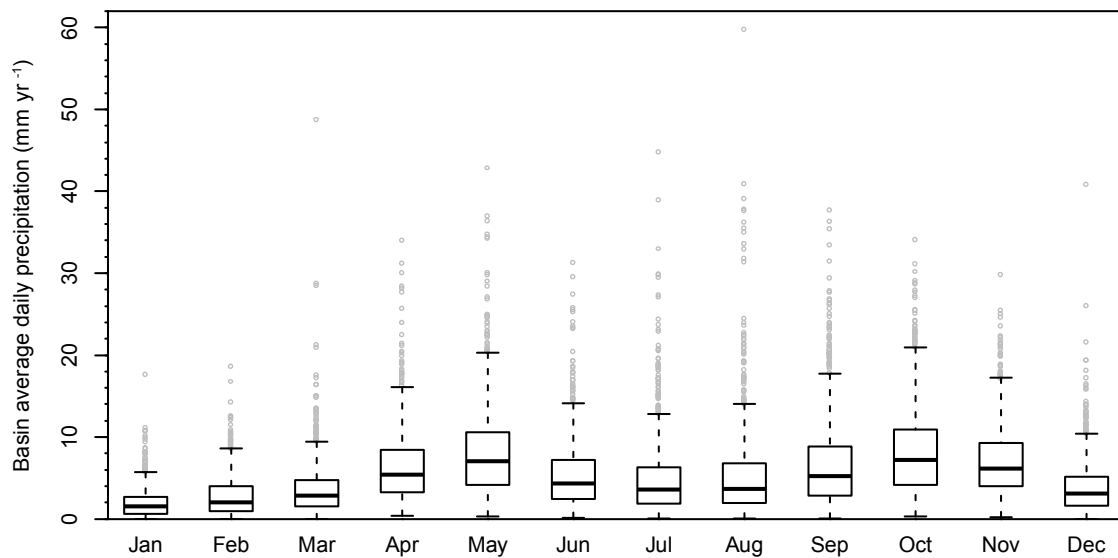


Figure 10. Boxplots of daily precipitation for the PRINCETON 1979-2008 series averaged over the Magdalena basin and grouped per month ( $n \approx 913$ ). The outliers are defined as values more than 1.5 times the IQR away from Q3.

### 4.1.2.2 Temperature and reference evapotranspiration

Although temperature when compared to most climates around the world is very constant in the Magdalena basin there is some intra-annual variation present (Figure 11). It is again very slight though, as the monthly medians vary within a range of less than 1 °C. Worth noticing are the warmer months of March and April and the higher variability of December and January.

The intra-annual pattern of reference evapotranspiration is a little more variable than that of temperature but, as it is determined using  $T_{\min}$  and  $T_{\max}$ , resembles the monthly variation in average daily temperature to a considerable degree. The remainder of the variation is caused



by variation in the difference between  $T_{\min}$  and  $T_{\max}$ . Most noticeable is the clear decrease in reference evapotranspiration in the period May to July caused by a decrease in difference between  $T_{\min}$  and  $T_{\max}$  (top panel of Figure 18).

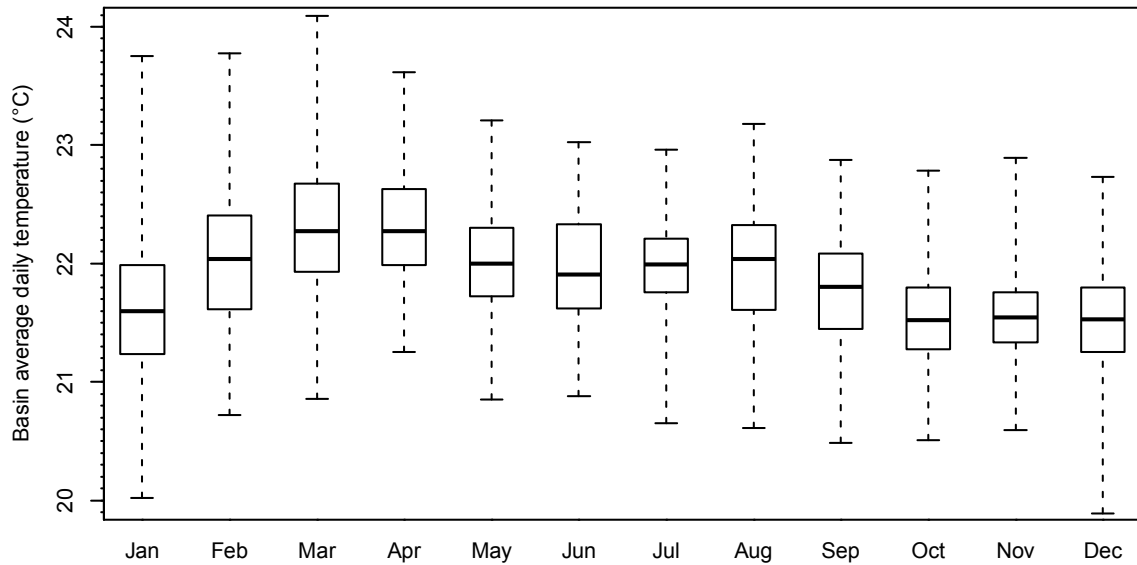


Figure 11. Boxplots of daily mean temperature for the PRINCETON 1979-2008 series averaged over the Magdalena basin and grouped per month ( $n = 10958$ , per month  $n \approx 913$ ).

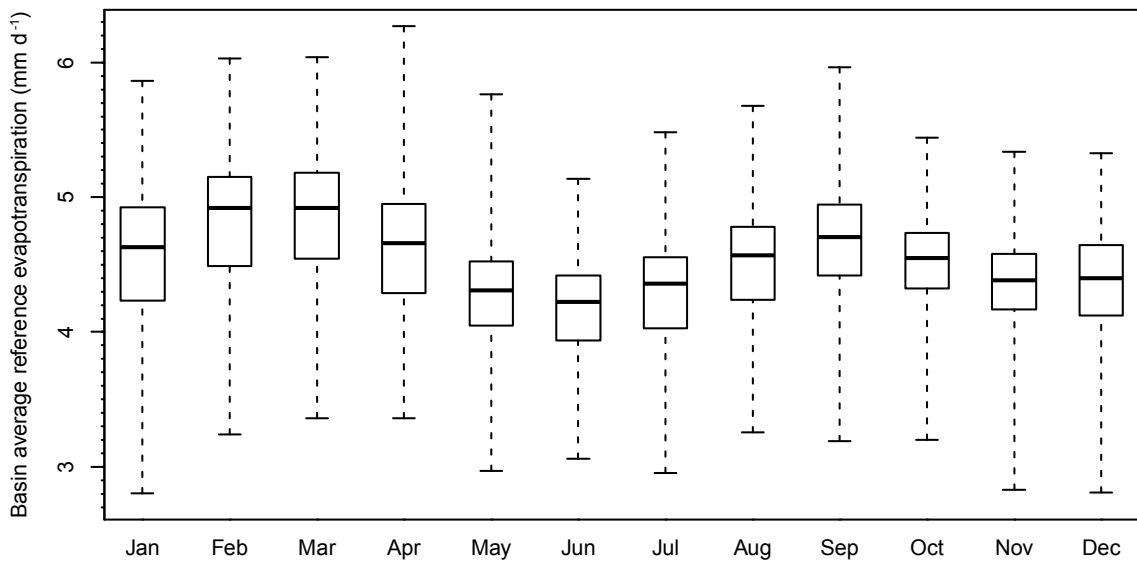


Figure 12. Boxplots of daily reference evapotranspiration as calculated from  $T_{\min}$  and  $T_{\max}$  for the PRINCETON 1979-2008 series averaged over the Magdalena basin and grouped per month ( $n = 10958$ , per month  $n \approx 913$ ).

#### 4.1.3 Precipitation return periods

Return levels and periods for basin average daily precipitation (Figure 13) were determined by using a Gumbel extreme value distribution approach (Alves and Neves, 2011). For every year the maximum precipitation value was selected, the 30 selected maxima were sorted according to their value, a Gumbel value was calculated and translated into return periods using its probability. To extrapolate the values to longer return periods a generalized extreme value



regression model based on maximum-likelihood was fitted to the values (Kaiser and Horenko, 2013).

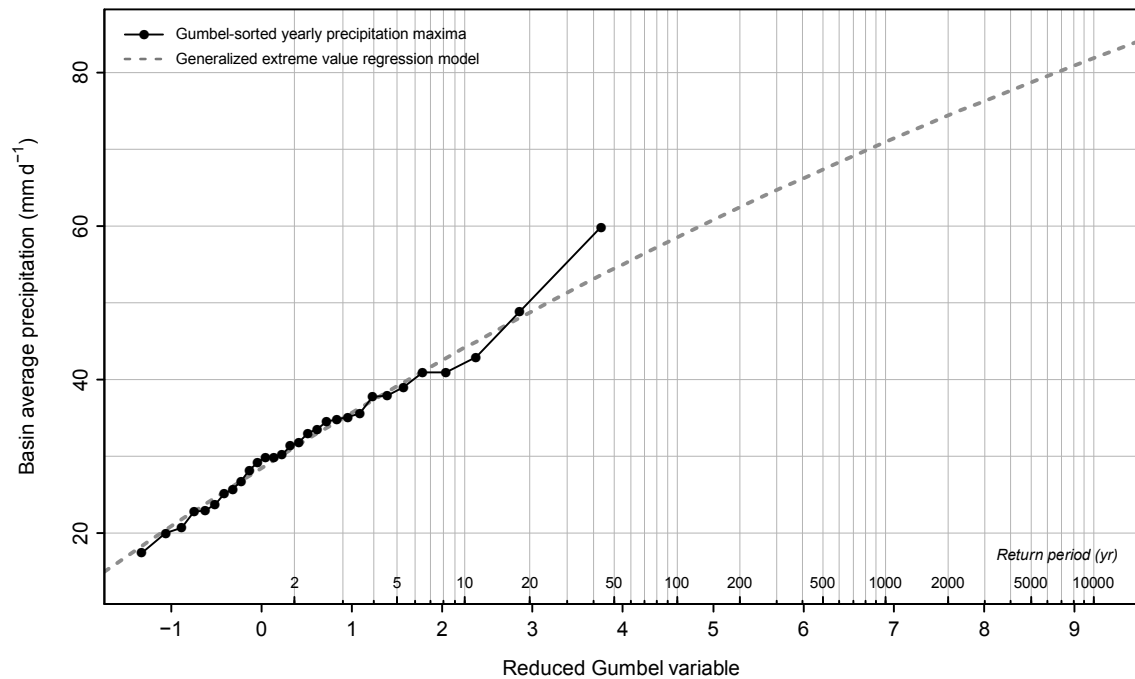


Figure 13. Return levels and periods of basin average daily precipitation for the PRINCETON 1979-2008 series as determined by using an extreme values distribution approach.

#### 4.1.4 Spatial distribution of precipitation

As the ITCZ moves throughout the year, the spatial distribution of precipitation in the Magdalena basin varies (Figure 14). In northern hemisphere's winter (fourth column) there is little precipitation but most rainfall occurs in the southern area of the basin. In spring the ITCZ moves north and the rain season's precipitation is concentrated in the center of the basin. In summer the ITCZ is at its most northern position, as is the rain. The second rain season in autumn concentrates itself a bit more southwards again.

When comparing the spatial characteristics of precipitation for the two rain seasons it can be noted that they are considerably similar. The second rain season is more pronounced with heavy precipitation (>800 mm) that is quite well distributed over the basin, but in terms of overall spatial distribution of rainfall amounts larger than ~550 mm they are comparable.

#### 4.1.5 Spatial distribution of temperature and evapotranspiration

As already noted in section 4.1.1 and 4.1.2.2, temperature and consequently reference evapotranspiration are both very constant over the 30-year reference period and reasonably constant throughout the year. This temporal invariability is also very clear from Figure 14.

Spatially there is significant variability, however, due the lapse correction that was applied during the downscaling of the PRINCETON temperature data. The terrain pattern of mountains and plains can be clearly noted due to this.

The Northern Andes range and its foothills lie in the southern area of Magdalena basin and have high peaks up to ~4500 m. This results in a high spatial variability of daily average temperature values within the basin. Temperature ranges from about 0 to 30 °C and reference



evaporation from about 600 to 2000 mm yr<sup>-1</sup>. The northern area of the Magdalena basin, towards the outflow of the Magdalena River in the Caribbean Sea, consists of lowland river plains and hence encounters the highest temperatures en evapotranspiration in the entire basin.

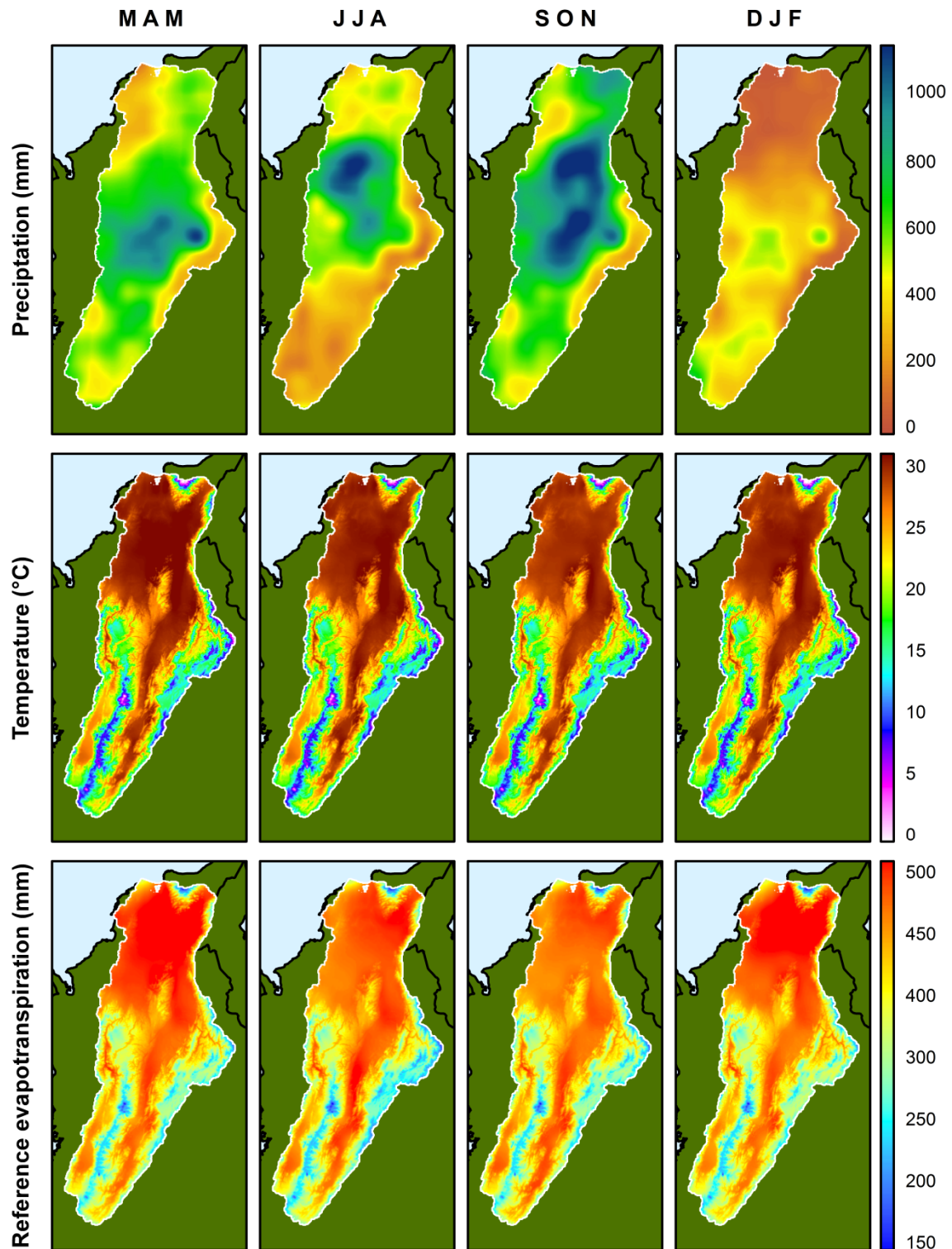


Figure 14. Seasonal maps of the PRINCETON 1979-2008 series for precipitation, temperature and estimated reference evapotranspiration.

## 4.2 Future changes in climate

The changes in future precipitation and temperature that are present within the GCMs are evaluated by calculating the differences between the PRINCETON reference series and their ADC-transformed counterparts. Evaluation of the transformed series instead of direct evaluation of the GCM control and future signals has the advantage that the bias correction of the ADC transformation method is incorporated in the results.

The long term variation and trends of the transformed series will not be significantly different from those of the reference series and are therefore not provided here. The annual trend will not change because the scaling of daily observations is performed using the same 30-year monthly statistics for every year. The intra-annual variation will change, however, and is therefore mainly used for the evaluation.

### 4.2.1 Changes in precipitation distribution

In terms of precipitation it is useful to look at the respective changes within its distribution for every calendar month compared to the reference situation, as a non-linear transformation was applied and non-linear shifts of the distribution are therefore expected. It is chosen to again use precipitation quantiles of five day sums for the evaluation ( $P_{30}$ ,  $P_{60}$  and  $P_{90}$ ), which were also used for the ADC method (section 3.3).

#### 4.2.1.1 Evaluated GCM ensemble

To visualize the differences that the use of different GCMs or even different realizations and parameterizations of the same model can have on the transformation results their ranges are plotted in Figure 15. It shows the total ranges of relative changes that were found for all seven analyzed GCM realizations for the two different RCPs and future periods. The top panel shows the quantiles for the 1979-2008 reference period.

As can be noted, there are considerable differences possible between different GCMs and realizations. Looking at  $P_{60}$  and  $P_{90}$  the maximum ranges found vary over months but can go up to 20-30%, which is quite significant. The range of differences found for  $P_{30}$  are even higher but that could be due to the fact that the lower part of the distribution is less accurately transformed as the transformation is based on  $P_{60}$  and  $P_{90}$  (Kraaijenbrink, 2013). The differences present between the realizations reinforce that any conclusions that are drawn from GCM analyses must be done carefully

#### 4.2.1.2 Selected GCM realizations

In the framework of the project two GCMs realizations were selected for two RCPs and two future periods (section 3.2.3). The differences found in  $P_{30}$ ,  $P_{60}$  and  $P_{90}$  for these scenarios compared to the reference period are shown in Figure 16 and Figure 17. Directly noticeable is that the three quantiles all have clearly different change values. This shows that indeed the non-linearity present in the GCM signal was applied to the reference series and that the monthly precipitation distributions have changed compared to the reference series.

Apparent for all scenarios is that the precipitation for December to February, i.e. the low precipitation season, will increase considerably. Remarkably, the increase in  $P_{90}$  is lower than  $P_{60}$  and  $P_{30}$ , meaning that the variability will decrease and a steadier precipitation regime will prevail, albeit with more precipitation in general. This is potentially good for water availability during these low precipitation months.



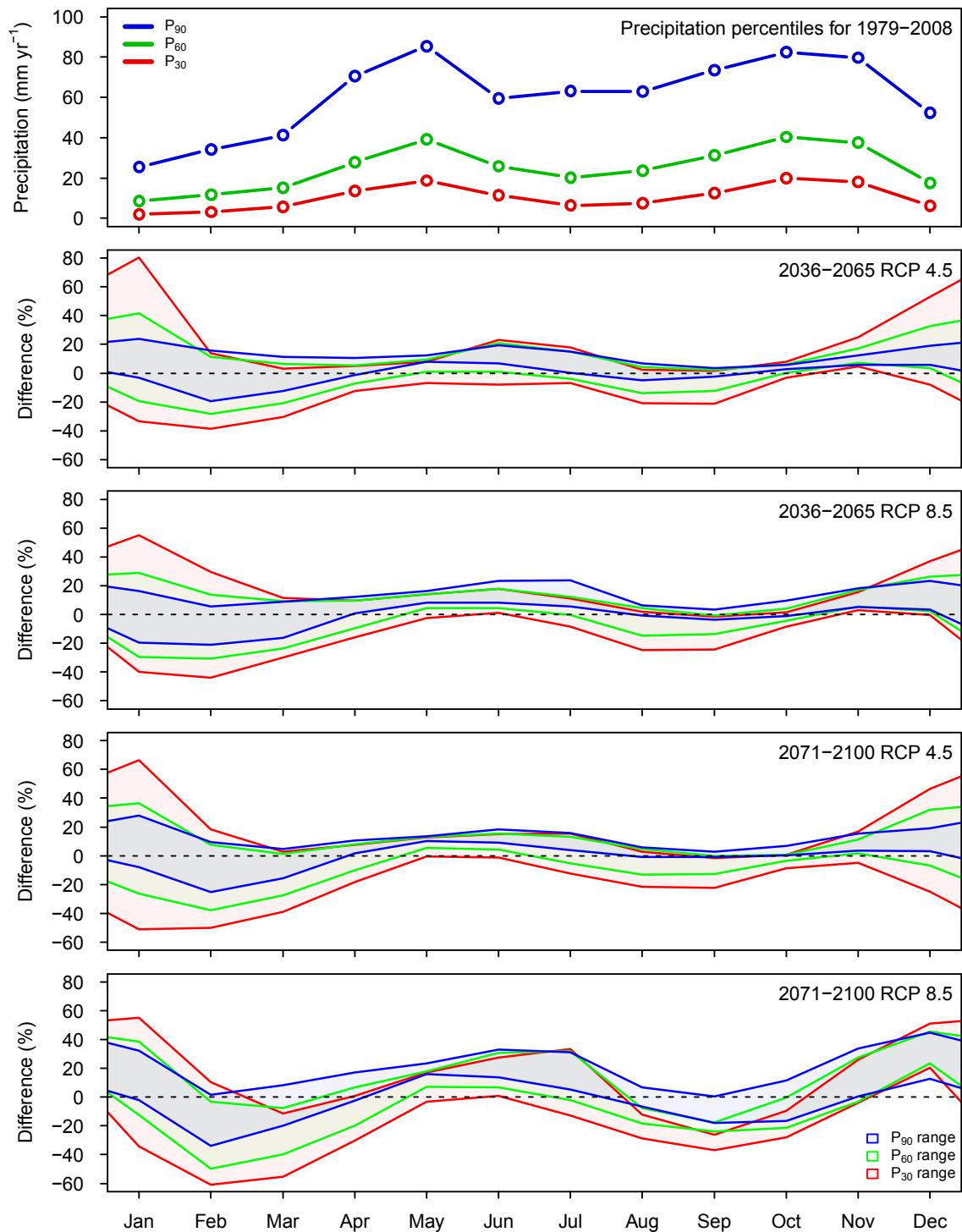


Figure 15. Basin average changes in  $P_{30}$ ,  $P_{60}$  and  $P_{90}$  of five day sums for the transformed PRINCETON series. The top panel shows the reference situation. The bottom panels show the percentage-wise range of changes found for the transformed PRINCETON series considering all seven examined GCM realizations (Table 4).



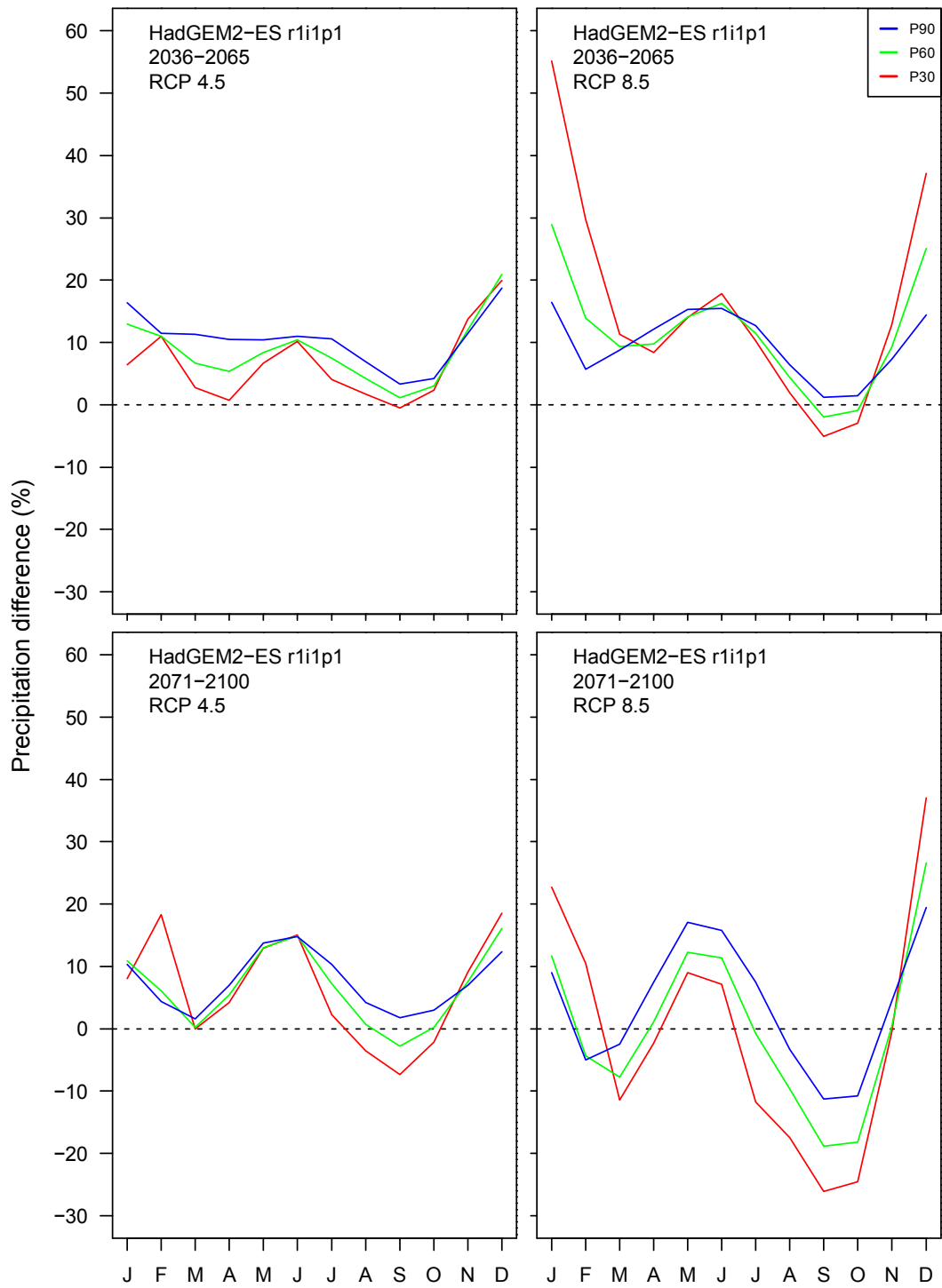


Figure 16. Basin average changes with respect to the reference series in  $P_{30}$ ,  $P_{60}$  and  $P_{90}$  of five day sums for the PRINCETON series that were transformed with HadGEM2-ES r1i1p1 realization.



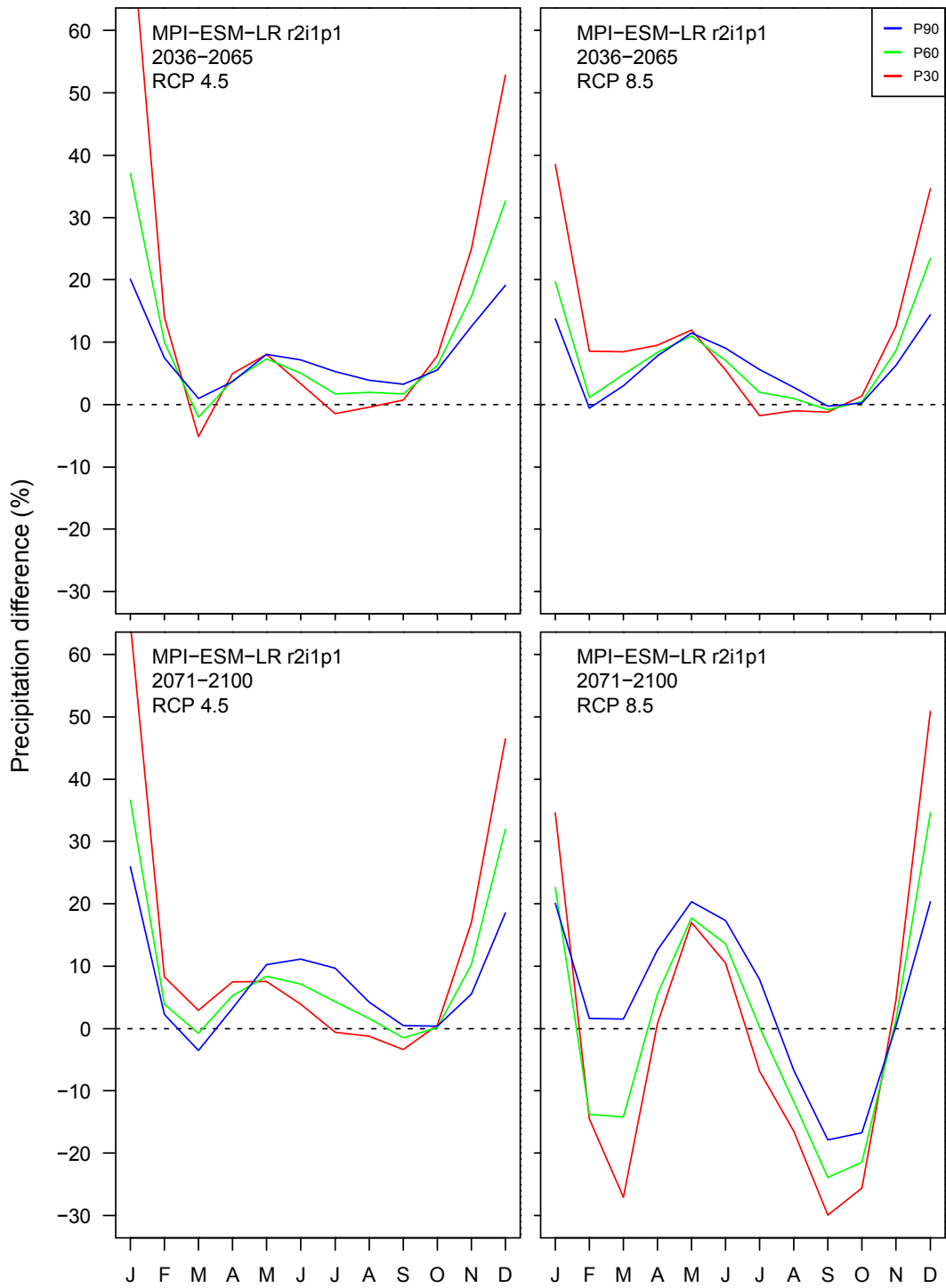


Figure 17. Basin average changes with respect to the reference series in  $P_{30}$ ,  $P_{60}$  and  $P_{90}$  of five day sums for the PRINCETON series that were transformed with the MPI-ESM-LR r2i1p1 realization.



An import signal to note present in most scenarios is that the precipitation of the second rain season, i.e. October-November, will either remain relatively similar or encounter considerable decreases. Especially in the EOC RCP 8.5 scenarios this is quite severe, with a decrease in  $P_{90}$  of up to ~20%. This case could, however, result in a decreased flood risk for that season. A similar pattern is present for February and March as well, although less pronounced.

Contrarily, in practically every scenario the first rain season intensifies. Depending on the scenario  $P_{90}$  increases with 5% to 20%. As the precipitation in this season has already been the cause of major inundations in the last decade, future flooding frequency and severity will likely increase if no mitigating measures are conducted.

For most months the precipitation distribution will change, i.e. variability will either decrease or increase. In the months where variability increases the distribution will become more shifted and skewed to the right, similarly as the sketch of the future precipitation in Figure 6 shows. This means more precipitation in general, a higher frequency of heavy rains as well as more severe heavy rains. This of course can become of major importance in the basin and hydrological modelling must provide with answers about the consequences for the discharge regimes in the Magdalena basin.

#### 4.2.2 Changes in temperature

Figure 18 shows the ranges found for all evaluated GCM realizations, similarly as Figure 15. It shows that changes in future temperature are again much more constant than the changes in precipitation. The realizations generally have good agreement as they only span a minor range of about 0.5 °C in the MOC scenarios and about 1.0 °C in the EOC scenarios. Temperature increases with about 2 and 2.5 °C throughout the year for RCP 4.5 and 8.5 respectively in the MOC. The EOC values clearly reflect the large continuous increase in radiation of RCP 8.5 (Figure 5) compared to that of RCP 4.5. They have a factor two difference: an increase of about 5.0 and 2.5 °C respectively.

The changes in temperature are clearly more directly related to the RCPs than the changes in precipitation. Apparently the changes in radiation at the top of atmosphere that are prescribed by the RCPs have a more direct influence on air, land and ocean temperatures, despite the existence of complicated greenhouse gas and ocean dynamics.

#### 4.2.3 Changes in reference evapotranspiration

Reference evapotranspiration as calculated in this project will not change very much in the future scenarios. The use of the modified Hargreaves method (Equation 2) causes reference evapotranspiration to change only if extra-terrestrial radiation changes or if the difference between  $T_{\min}$  and  $T_{\max}$  temperature will increase or decrease. An increase in their difference will increase reference evapotranspiration and vice versa. An equal increase of both will not influence the evapotranspiration.

Figure 18 shows that  $T_{\min}$  and  $T_{\max}$  will increase rather equally overall. The only real noticeable difference for all scenarios are the months September and October. Here  $T_{\max}$  will increase more than  $T_{\min}$ , which leads to a slightly increased evapotranspiration in those months. Note that these are also the months where the largest decreases in precipitation are expected and water balance will be affected even more.



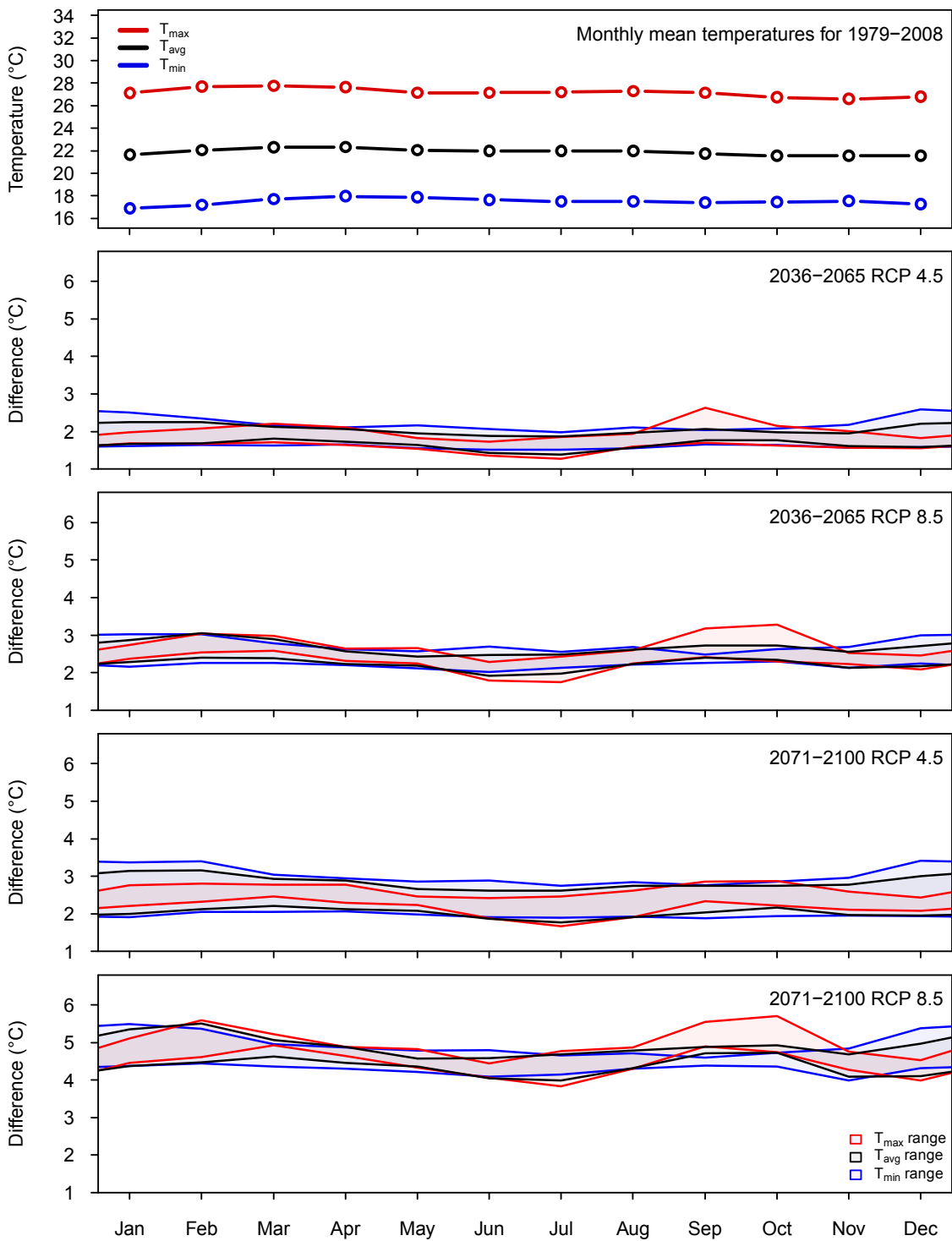


Figure 18. Basin average changes in minimum, average and maximum temperature for the transformed PRINCETON data. The top panel shows the reference situation. The bottom panels show the range of changes found for the transformed PRINCETON series considering all seven examined GCM realizations (Table 4).



#### 4.2.4 Return period changes

Return periods for the future scenarios (Figure 19) were determined similarly as for the reference period in section 4.1.3. The return levels of the MPI-ESM-LR RCP 8.5 model run show the largest extremes for both the MOC as EOC, likely due to its large increase of precipitation during the first rain season (section 4.2.1.2). In general it is clear that for all scenarios an increase of the extreme values can be expected of about 5 to 20% compared to the reference data. This is a significant increase and it will likely affect flooding risks.

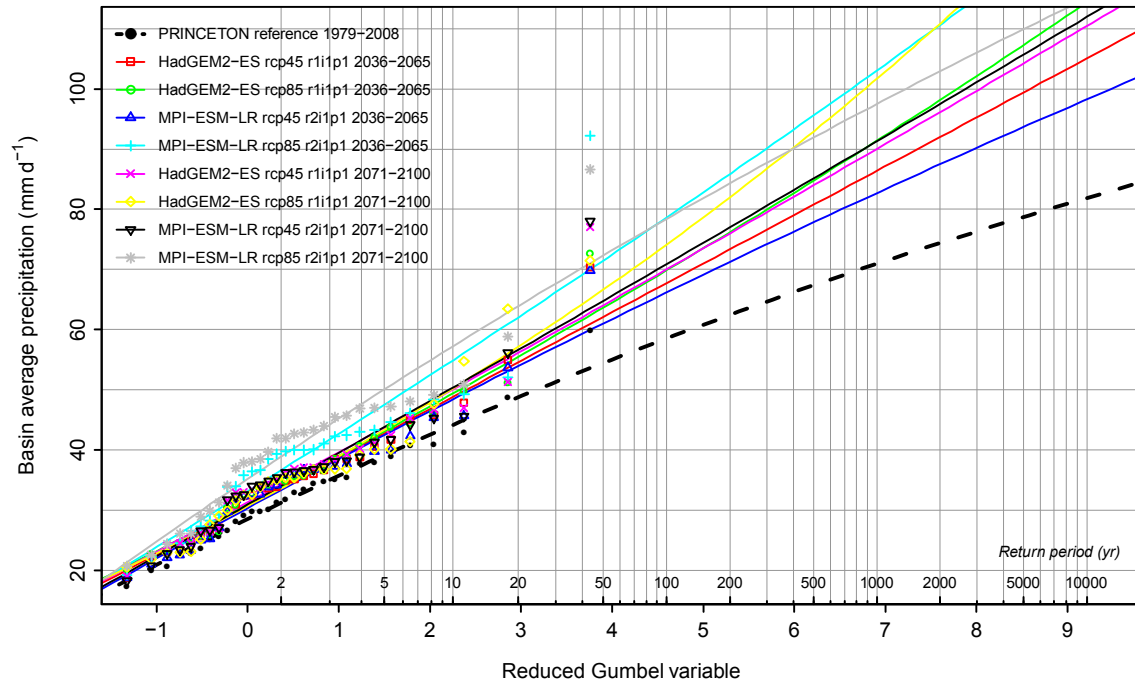


Figure 19. Return periods and return levels for basin average precipitation of the future scenarios.

#### 4.2.5 Spatial changes

Besides the basin-wide changes that the climate variables will encounter in the future, there will of course also be a spatial variability of these changes, which can be different for each future scenario. To visualize this, maps were produced that show the spatial changes for two specific EOC scenarios: MPI-ESM-LR RCP 4.5 and HadGEM2-ES RCP 8.5 (Figure 20 and Figure 21 respectively). For temperature and reference evapotranspiration there are not that many differences between the two scenarios, mainly differences in the quantity of change. For precipitation, however, there are clear spatial differences. There is also some agreement, for instance the occurrence of precipitation decreases in the south and east of the basin.

Also, for almost all seasons and model runs that are shown, there is a relatively consistent and considerable decrease found in the precipitation of the northern coastal area. Although it is possibly valid to a certain degree it could be for a large part due to influences of and interplays between the GCM and PRINCETON grid cells that cover the Caribbean Sea and the coastal part of the continent. Land and ocean data is likely to have been mixed here during interpolation, leading to inaccuracies as the two water cycles are very different.

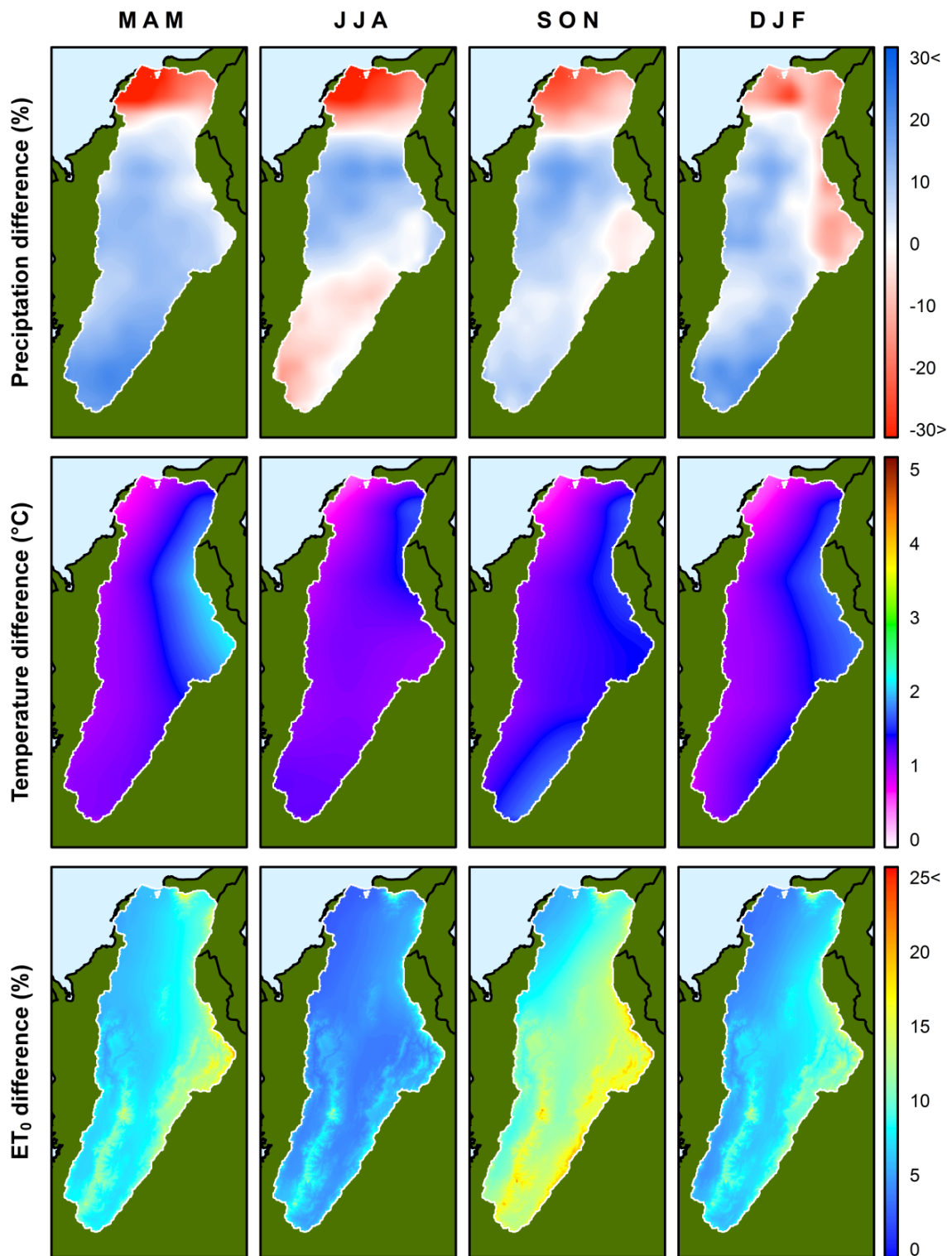


Figure 20. Spatial variability of the differences in seasonal statistics found between the reference PRINCETON 1979-2008 series and the series transformed using the MPI-ESM-LR RCP 4.5 realization for 2071-2100.

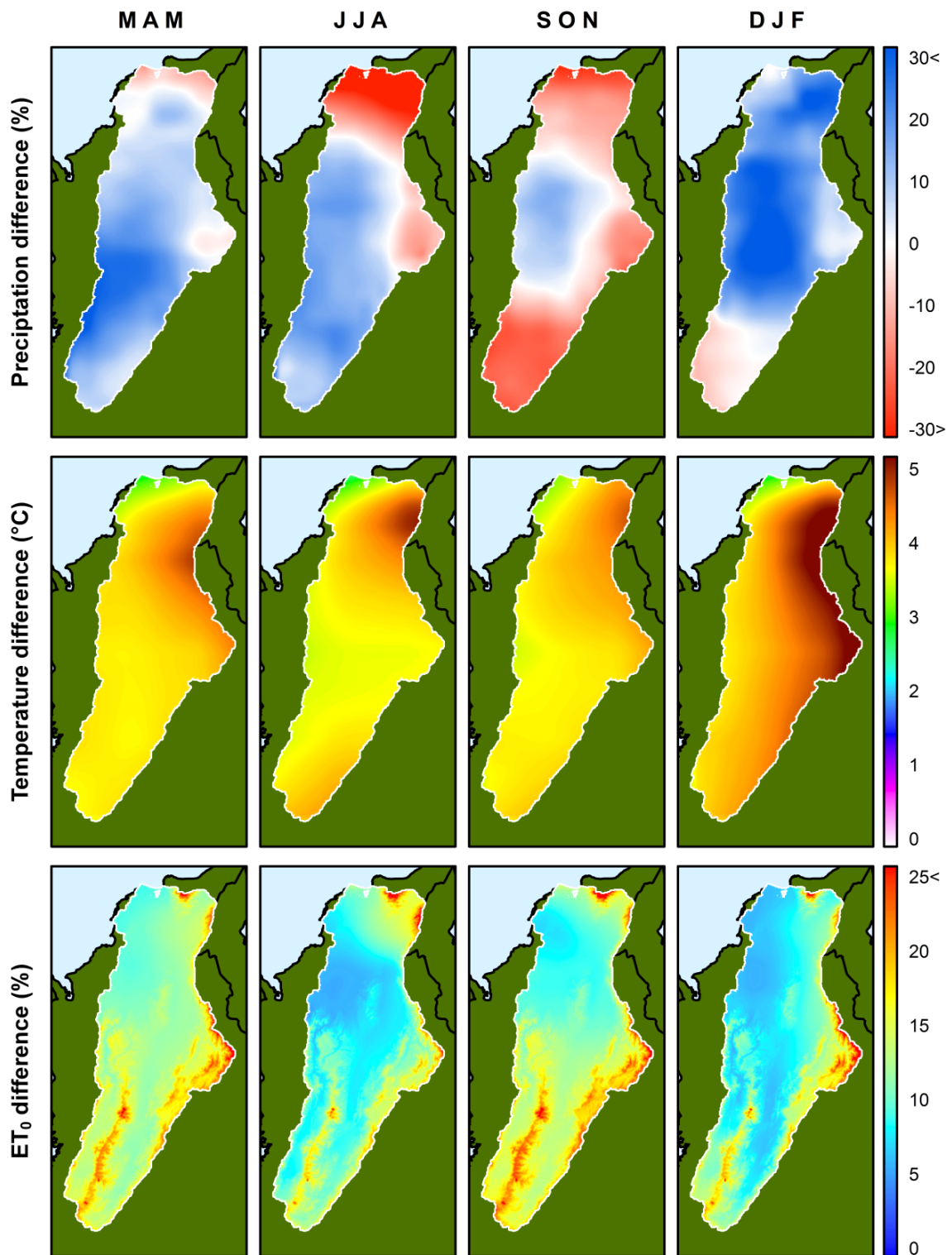


Figure 21. Spatial variability of the differences in seasonal statistics found between the reference PRINCETON 1979-2008 series and the series transformed using the HadGEM2-ES RCP 8.5 realization for 2071-2100.

## 5 References

- Adler, R. F., Huffman, G. J., Chang, A., Ferraro, R., Xie, P., Janowiak, J., Rudolf, B., Schneider, U., Curtis, S., Bolvin, D., Gruber, A., Susskind, J., Arkin, P. and Nelkin, E.: The Version-2 Global Precipitation Climatology Project ( GPCP ) Monthly Precipitation Analysis ( 1979 – Present ), *J. Hydrometeorol.*, 4, 1147–1167, 2003.
- Alves, I. and Neves, C.: Extreme value distributions, in *International Encyclopedia of Statistical Science*, pp. 493–496, Springer Berlin Heidelberg, Berlin., 2011.
- Burrough, P. A. and McDonnell, R.: *Principles of geographical information systems*, Oxford university press Oxford., 1998.
- Compo, G. P., Whitaker, J. S., Sardeshmukh, P. D., Matsui, N., Allan, R. J., Yin, X., Gleason, B. E., Vose, R. S., Rutledge, G., Bessemoulin, P., Brönnimann, S., Brunet, M., Crouthamel, R. I., Grant, a. N., Groisman, P. Y., Jones, P. D., Kruk, M. C., Kruger, a. C., Marshall, G. J., Maugeri, M., Mok, H. Y., Nordli, Ø., Ross, T. F., Trigo, R. M., Wang, X. L., Woodruff, S. D. and Worley, S. J.: The Twentieth Century Reanalysis Project, *Q. J. R. Meteorol. Soc.*, 137(654), 1–28, doi:10.1002/qj.776, 2011.
- Dee, D.: *Toward a consistent reanalysis of the climate system*, 2013.
- Dee, D. P., Uppala, S. M., Simmons, a. J., Berrisford, P., Poli, P., Kobayashi, S., Andrae, U., Balmaseda, M. a., Balsamo, G., Bauer, P., Bechtold, P., Beljaars, a. C. M., van de Berg, L., Bidlot, J., Bormann, N., Delsol, C., Dragani, R., Fuentes, M., Geer, a. J., Haimberger, L., Healy, S. B., Hersbach, H., Hólm, E. V., Isaksen, L., Kållberg, P., Köhler, M., Matricardi, M., McNally, a. P., Monge-Sanz, B. M., Morcrette, J.-J., Park, B.-K., Peubey, C., de Rosnay, P., Tavolato, C., Thépaut, J.-N. and Vitart, F.: The ERA-Interim reanalysis: configuration and performance of the data assimilation system, *Q. J. R. Meteorol. Soc.*, 137(656), 553–597, doi:10.1002/qj.828, 2011.
- Droogers, P. and Allen, R. G.: Estimating reference evapotranspiration under inaccurate data conditions, *Irrig. Drain. Syst.*, 16(1), 33–45, 2002.
- Great Rivers Partnership: Magdalena River Basin, , 1 [online] Available from: <http://www.greatriverspartnership.org/en-us/southamerica/magdalena/pages/default.aspx> (Accessed 5 May 2014), 2014.
- Harris, I., Jones, P. D., Osborn, T. J. and Lister, D. H.: Updated high-resolution grids of monthly climatic observations - the CRU TS3.10 Dataset, *Int. J. Climatol.*, doi:10.1002/joc.3711, 2013.
- Huffman, G. J., Adler, R. F., Arkin, P., Chang, A., Ferraro, R., Gruber, A., Janowiak, J., Mcnab, A., Rudolf, B. and Schneider, U.: The Global Precipitation Climatology Project ( GPCP ) Combined Precipitation Dataset, *Bull. Am. Meteorol. Soc.*, 78(1), 5–20, 1997.
- IDEAM: Colombia: Primera comunicación nacional ante la Convención Marco de las Naciones Unidas sobre el Cambio Climático, Instituto de Hidrología, Meteorología y Estudios Ambientales (IDEAM), Bogotá., 2001.
- IDEAM: Colombia: Segunda comunicación nacional ante la Convención Marco de las Naciones Unidas sobre el Cambio Climático, Instituto de Hidrología, Meteorología y Estudios Ambientales (IDEAM), Bogotá., 2010.
- IIASA: RCP Database., 2013.
- Kaiser, O. and Horenko, I.: On inference of statistical regression models for extreme events based on incomplete observation data, , (2), 1–33, 2013.
- Kalnay, E., Kanamitsu, M., Kistler, R., Collins, W., Deaven, D., Gandin, L., Iredell, M., Saha, S., White, G., Woollen, J., Zhu, Y., Chelliah, M., Ebisuzak, W., Higgins, W., Janowiak, J., Mo, K. C., Ropelewski, C., Wang, J., Leetmaa, A., Reynolds, R., Jenne, R. and Joseph, D.: The NCEP/NCAR 40-Year Reanalysis Project, *Bull. Am. Meteorol. Soc.*, 77(3), 437 – 471, 1996.
- Kanamitsu, M., Ebisuzaki, W., Woollen, J., Yang, S.-K., Hnilo, J. J., Fiorino, M. and Potter, G. L.: NCEP–DOE AMIP-II Reanalysis (R-2), *Bull. Am. Meteorol. Soc.*, 83(11), 1631–1643, doi:10.1175/BAMS-83-11-1631, 2002.
- Kraaijenbrink, P. D. A.: Advanced Delta Change method: Extension of an application to CMIP5 GCMs, De Bilt., 2013.
- Lorenz, C. and Kunstmann, H.: The Hydrological Cycle in Three State-of-the-Art Reanalyses: Intercomparison and Performance Analysis, *J. Hydrometeorol.*, 13(5), 1397–1420, doi:10.1175/JHM-D-11-088.1, 2012.
- Lutz, A., Terink, W., Droogers, P., Immerzeel, W. and Piman, T.: Development of baseline climate data set and trend analysis in the Mekong Basin, Wageningen., 2014.
- NCAR: *The Climate Data Guide*, 2013.
- New, M., Hulme, M. and Jones, P.: Representing Twentieth-Century Space – Time Climate Variability . Part I : Development of a 1961 – 90 Mean Monthly Terrestrial Climatology, *J. Clim.*, 12, 829–856, 1999.



- New, M., Hulme, M. and Jones, P.: Representing Twentieth-Century Space – Time Climate Variability . Part II : Development of 1901 – 96 Monthly Grids of Terrestrial Surface Climate, *J. Clim.*, 13, 2217–2238, 2000.
- NOAA: National Oceanic and Atmospheric Administration, Climate Prediction Center - Monitoring & Data: Ocean Niño Index Changes Description, [online] Available from: [http://www.cpc.ncep.noaa.gov/products/analysis\\_monitoring/ensostuff/ONI\\_change.shtml](http://www.cpc.ncep.noaa.gov/products/analysis_monitoring/ensostuff/ONI_change.shtml), 2014.
- PCMDI: Program For Climate Model Diagnosis and Intercomparison: Coupled Model Intercomparison Project Phase 5, [online] Available from: <http://cmip-pcmdi.llnl.gov/cmip5/> (Accessed 23 April 2014), 2014.
- Van Pelt, S. C., Beersma, J. J., Buishand, T. A., van den Hurk, B. and Kabat, P.: Future changes in extreme precipitation in the Rhine basin based on global and regional climate model simulations, *Hydrol. Earth Syst. Sci.*, 16, 4517–4530, 2012.
- Peubey, C., Hersbach, H., Poli, P., Simmons, A., Dee, D., Berrisford, P., Dragani, R., Komori, T., Laloyaux, P. and Tan, D.: The ERA-20CM twentieth century atmosphere model ensemble, *EMS Annu. Meet. Abstr.*, 10(13th EMS / 11th ECAM), 2013, 2013.
- Poveda, G., Álvarez, D. M. and Rueda, Ó. a.: Hydro-climatic variability over the Andes of Colombia associated with ENSO: a review of climatic processes and their impact on one of the Earth's most important biodiversity hotspots, *Clim. Dyn.*, 36(11-12), 2233–2249, 2010.
- Rienecker, M. M., Suarez, M. J., Gelaro, R., Todling, R., Bacmeister, J., Liu, E., Bosilovich, M. G., Schubert, S. D., Takacs, L., Kim, G.-K., Bloom, S., Chen, J., Collins, D., Conaty, A., da Silva, A., Gu, W., Joiner, J., Koster, R. D., Lucchesi, R., Molod, A., Owens, T., Pawson, S., Pegion, P., Redder, C. R., Reichle, R., Robertson, F. R., Ruddick, A. G., Sienkiewicz, M. and Woollen, J.: MERRA: NASA's Modern-Era Retrospective Analysis for Research and Applications, *J. Clim.*, 24(14), 3624–3648, doi:10.1175/JCLI-D-11-00015.1, 2011.
- Saha, S., Moorthi, S., Pan, H.-L., Wu, X., Wang, J., Nadiga, S., Tripp, P., Kistler, R., Woollen, J., Behringer, D., Liu, H., Stokes, D., Grumbine, R., Gayno, G., Wang, J., Hou, Y.-T., Chuang, H.-Y., Juang, H.-M. H., Sela, J., Iredell, M., Treadon, R., Kleist, D., Van Delst, P., Keyser, D., Derber, J., Ek, M., Meng, J., Wei, H., Yang, R., Lord, S., Van Den Dool, H., Kumar, A., Wang, W., Long, C., Chelliah, M., Xue, Y., Huang, B., Schemm, J.-K., Ebisuzaki, W., Lin, R., Xie, P., Chen, M., Zhou, S., Higgins, W., Zou, C.-Z., Liu, Q., Chen, Y., Han, Y., Cucurull, L., Reynolds, R. W., Rutledge, G. and Goldberg, M.: The NCEP Climate Forecast System Reanalysis, *Bull. Am. Meteorol. Soc.*, 91(8), 1015–1057, doi:10.1175/2010BAMS3001.1, 2010.
- Schneider, U., Becker, A., Finger, P., Meyer-Christoffer, A., Ziese, M. and Rudolf, B.: GPCP's new land surface precipitation climatology based on quality-controlled in situ data and its role in quantifying the global water cycle, *Theor. Appl. Climatol.*, 26, doi:10.1007/s00704-013-0860-x, 2013.
- Sheffield, J., Goteti, G. and Wood, E. F.: Development of a 50-Year High-Resolution Global Dataset of Meteorological Forcings for Land Surface Modeling, *J. Clim.*, 19(13), 3088–3111, doi:10.1175/JCLI3790.1, 2006.
- Taylor, K. E., Stouffer, R. J. and Meehl, G. A.: An overview of CMIP5 and the experiment design, *Bull. Am. Meteorol. Soc.*, 93(4), 485, 2012.
- Uppala, S. M., Kållberg, P. W., Simmons, a. J., Andrae, U., Bechtold, V. D. C., Fiorino, M., Gibson, J. K., Haseler, J., Hernandez, A., Kelly, G. a., Li, X., Onogi, K., Saarinen, S., Sokka, N., Allan, R. P., Andersson, E., Arpe, K., Balmaseda, M. a., Beljaars, a. C. M., Berg, L. Van De, Bidlot, J., Bormann, N., Caires, S., Chevallier, F., Dethof, A., Dragosavac, M., Fisher, M., Fuentes, M., Hagemann, S., Hólm, E., Hoskins, B. J., Isaksen, I., Janssen, P. a. E. M., Jenne, R., McNally, a. P., Mahfouf, J.-F., Morcrette, J.-J., Rayner, N. a., Saunders, R. W., Simon, P., Sterl, A., Trenberth, K. E., Untch, A., Vasiljevic, D., Viterbo, P. and Woollen, J.: The ERA-40 re-analysis, *Q. J. R. Meteorol. Soc.*, 131(612), 2961–3012, 2005.
- Utrecht University: PCRaster 4.0., 2013.
- Ward, P. J., Eisner, S., Flörke, M., Dettinger, M. D. and Kummu, M.: Annual flood sensitivities to El Niño–Southern Oscillation at the global scale, *Hydrol. Earth Syst. Sci.*, 18(1), 47–66, doi:10.5194/hess-18-47-2014, 2014.
- Willmott, C. J. and Rowe, C. M.: Climatology of the terrestrial seasonal water cycle, *J. Climatol.*, 5, 589–606, 1985.
- Xie, P., Chen, M., Yang, S., Yatagai, A., Hayasaka, T., Fukushima, Y. and Liu, C.: A Gauge-Based Analysis of Daily Precipitation over East Asia, *J. Hydrometeorol.*, 8(3), 607–626, doi:10.1175/JHM583.1, 2007.